Atmos. Chem. Phys., 10, 5641–5662, 2010
www.atmos-chem-phys.net/10/5641/2010/
doi:10.5194/acp-10-5641-2010

Atmospheric Chemistry and Physics

Spatial distribution and interannual variation of surface PM_{10} concentrations over eighty-six Chinese cities

W. J. Qu[1,2], R. Arimoto[3,*], X. Y. Zhang[2], C. H. Zhao[1], Y. Q. Wang[2], L. F. Sheng[1], and G. Fu[1]

[1]Physical Oceanography Laboratory, Ocean-Atmosphere Interaction and Climate Laboratory, Department of Marine Meteorology, College of Physical and Environmental Oceanography, Ocean University of China, 238 Songling Rd., Laoshan District, Qingdao 266100, China
[2]Key Laboratory of Atmospheric Chemistry, Centre for Atmosphere Watch and Services (CAWAS), Chinese Academy of Metrological Sciences, China Meteorological Administration, 46 Zhong-Guan-Cun S. Ave., Beijing 100081, China
[3]Carlsbad Environmental Monitoring and Research Center, New Mexico State University, Carlsbad, New Mexico, USA
[*]retired

Received: 5 September 2009 – Published in Atmos. Chem. Phys. Discuss.: 2 November 2009
Revised: 21 May 2010 – Accepted: 18 June 2010 – Published: 29 June 2010

Abstract. The spatial distribution of the aerosols over 86 Chinese cities was reconstructed from air pollution index (API) records for summer 2000 to winter 2006. PM_{10} (particulate matter $\leq$10 µm) mass concentrations were calculated for days when PM_{10} was the principal pollutant, these accounted for 91.6% of the total 150 428 recorded days. The 83 cities in mid-eastern China (100° E to 130° E) were separated into three latitudinal zones using natural landscape features as boundaries. Areas with high PM_{10} level in northern China (127 to 192 µg m^{-3}) included Urumchi, Lanzhou-Xining, Weinan-Xi'an, Taiyuan-Datong-Yangquan-Changzhi, Pingdingshan-Kaifeng, Beijing-Tianjin-Shijiazhuang, Jinan, and Shenyang-Anshan-Fushun; in the middle zone, high PM_{10} (119–147 µg m^{-3}) occurred at Chongqing-Chengdu-Luzhou, Changsha-Wuhan, and Nanjing-Hangzhou; in the southern zone, only four cities (Qujing, Guiyang, Guangzhou and Shaoguan) showed PM_{10} concentration $>$80 µg m^{-3}. The median PM_{10} concentration decreased from 108 µg m^{-3} for the northern cities to 95 µg m^{-3} and 55 µg m^{-3} for the middle and southern zones, respectively. PM_{10} concentration and the APIs both exhibited wintertime maxima, summertime minima, and the second highest values in spring. PM_{10} showed evidence for a decreasing trend for the northern cities while in the other zones urban PM_{10} levels fluctuated, but showed no obvious change over time. The spatial distribution of PM_{10} was compared with the emissions, and the relationship between the surface PM_{10} concentration and the aerosol optical depth (AOD) was also discussed.

Correspondence to: W. J. Qu
(quwj@ouc.edu.cn)

1 Introduction

The atmospheric aerosol plays an important role in visibility impairment (Watson, 2002), and studies of potential aerosol effects on climate have become of increasing interest following the pioneering work of Twomey (1977) and Charlson et al. (1992). Concerns over adverse influences of particulate matter (PM) on human health (Pope et al., 1995; Tie et al., 2009b) have added to the scientific and public interest in aerosol particles (hereinafter, simply aerosols).

Defining a representative aerosol distribution is essential for understanding the aerosols' effects on climate, especially over regional scales. However, this is challenging because the atmospheric aerosol shows marked spatial and temporal variations owing to the relatively short residence times of the particles and the heterogeneity of their sources (Kaufman et al., 2002). Aerosol distributions over the continent are generally regional because of the diversity in emissions (especially anthropogenic sources), unevenness in population density, and variations in terrain, which can concentrate air pollutants or enhance their dispersion. In this context, gradients in aerosol concentrations obviously exist, and these result in differences in the aerosols' effects. For example, data from an aircraft study over the Los Angeles Basin revealed horizontal gradients in aerosol concentrations that could result in variability of more than 50% within a 5×5 km computational grid cell (Collins et al., 2000). Related studies over the tropical Indian Ocean indicated that gradients in aerosols could lead to an inter-hemispheric difference in the solar heating (Rajeev and Ramanathan, 2001). Along these same lines, a gradient in the aerosol optical depth (AOD) could lead to difference in the reduction of the noontime solar flux from as much as -38 W m^{-2} in the Arabian Sea to as little

as $-2\,W\,m^{-2}$ south of the Intertropical Convergence Zone, thus producing a strong north to south gradient in the climate forcing (Meywerk and Ramanathan, 1999). Recent research has confirmed a strong latitudinal gradient in the total aerosol and black carbon (BC) over the Bay of Bengal with both decreasing rapidly from north to south (Nair et al., 2008). In addition to these latitudinal aerosol gradients, a strong west-to-east gradient of BC has also been observed during research cruises along latitudes of 30° N and 35° N in the central Pacific Ocean; this was attributed to outflow from Asia (Kaneyasu and Murayama, 2000).

As for the health impacts of air pollution, the sources of air pollutants are mostly restricted to the earth's surface; the main exception to this is aircraft emission in the upper troposphere (Highwood and Kinnersley, 2006). Meanwhile, approximately 47% of the global population lives and works in urban areas, which are the most polluted parts of the planet. Investigations of surface air quality over urban areas and strategies for its improvement are therefore compelling.

China, a developing country with the world's largest population, has undergone rapid economic growth since economic reforms began in 1978. Along with urbanization and industrialization has come an increase in energy consumption, and this has brought with it growing concerns over air pollution. Investigations of the spatial distribution and interannual variations in the atmospheric aerosol and air pollutants are necessary to understand the aerosol's potential effects on atmospheric chemical process and climate, these are also essential for the development and implementation of effective air pollution control strategies.

There have been numerous ground-based studies of the aerosol in China, including measurements of the physical and/or chemical properties at remote sites (Tang et al., 1999; Li et al., 2000; Qu et al., 2008), regionally representative rural sites (Xu et al., 2002; Wang et al., 2004a; Zhang et al., 2005) and urban sites in large and mega cities (Fang et al., 1999; Davis and Guo, 2000; He et al., 2001; Zhang et al., 2002; Cao et al., 2003; Ye et al., 2003; Ta et al., 2004; Duan et al., 2005, 2006; Wu et al., 2005; Zheng et al., 2005; Feng et al., 2006; Li et al., 2006, 2008; Meng et al., 2007; Chu et al., 2008; Deng et al., 2008a, 2008b). However, even taken together, the existing studies do not provide a systematic picture of the spatial distribution of the aerosol across China. This is in part because of the limited and discontinuous coverage of most observations and also because of difficulties in inter-comparing results among research groups who use different sampling instruments and analytical methods. As a result, there is limited information on the spatial distribution of the surface aerosol across the country.

On the other hand, information on the spatial distribution of aerosol over China has been obtained from radiation/optical measurement networks and satellite observations (Luo et al., 2000, 2001; Li et al., 2003; Wang et al., 2008). However, the columnar AOD or aerosol optical thickness (AOT) derived from these types of observations is influenced by many factors including the vertical structure and height of the atmospheric mixing layer; therefore, the characteristics and variations of the AOD/AOT will differ from those of the surface aerosol as will be discussed in Sect. 3.7 below.

Chan and Yao (2008) and Fang et al (2009) have reviewed the air pollution situations and air quality management practices in Chinese mega cities. Another review (Shao et al., 2006) indicated high levels of airborne PM in megacities such as Beijing, Shanghai, and Guangzhou as well as regional aerosol pollution in the vast region extending from the North China Plain (NCP) to the Yangtze River Delta region (YRD) and the heavily urbanized Pearl River Delta region (PRD). Tie et al. (2006a) characterized air pollution in Eastern China and the Eastern US to assess the differences between photochemical conditions in these two regions. Tie and Cao (2009a) discussed several crucial issues regarding aerosol pollution in the highly populated regions over China. A recent study (Song et al., 2009) characterized spatial and seasonal variations of PM_{10} concentrations (for 47 ground-based air quality monitoring sites) and the Moderate Resolution Imaging Spectroradiometer (MODIS) AOD over China during the period 2003–2005, but interannual variations were not considered.

As inhalable particulate pollutant, PM_{10} (PM with diameters $\leq 10\,\mu m$) is of primary concern for most Chinese cities, and PM_{10} is often reported as the principal pollutant (abbreviation as P_{prin} hereinafter, see below for definition) for urban areas that are monitored by the Environmental Protection Agency of China (EPA-China). In this paper we make use of 137845 daily air pollution index (API) records for eighty-six major cities (Fig. 1, Table 1) to estimate the concentrations of PM_{10} over urban areas in China. The results are then used to study the spatial variability of PM_{10} and to evaluate its seasonal and interannual variations.

The paper is organized as follows. In Section 2 we give an overview of methods and data. Section 3.1 presents occurrences of the air quality categories for the cities. Seasonal variations of the APIs and PM_{10} are presented in Section 3.2, and the influence of Asian dust on the springtime APIs is presented in Section 3.3. Section 3.4 and 3.5 describe spatial distribution of urban PM_{10} concentration versus emissions and precipitation as well as the broad pattern of latitudinal and longitudinal gradients in PM_{10} level for the cities; Section 3.6 presents interannual variation trends in urban PM_{10} for northern, middle and southern China. Section 3.7 presents comparison of PM_{10} variations with AOD/AOT results, and the factors that influence the relationships between PM_{10} and AOD/AOT are also discussed. Section 4 finally gives conclusions.

Table 1. Locations, groups and air pollution index (API) data available period of the eighty-six cities in China.

Group (Representative area)	City	Latitude, Longitude	API data period[a]
G-1	Xining (XN)	36.62° N, 101.82° E	A
(Qinghai,	Shizuishan (SZS)	39.02° N, 106.22° E	C
Gansu and	Yinchuan (YC)	38.47° N, 106.22° E	A
Ningxia Province)	Lanzhou (LaZ)	36.05° N, 103.83° E	A
G-2	Baoji (BaJ)	34.35° N, 107.15° E	C
(Shaanxi Province)	Xi'an (XA)	34.25° N, 108.92° E	A
	Weinan (WN)	34.30° N, 109.30° E	C
G-3	Hohehot (HHT)	40.80° N, 111.63° E	A
(Inner Mongolian	Chifeng (CF)	42.17° N, 118.58° E	C
and Shanxi	Datong (DT)	40.12° N, 113.22° E	C
Province)	Taiyuan (TY)	37.85° N, 112.55° E	A
	Yangquan (YQ)	37.51° N, 113.34° E	C
	Changzhi (CZ)	36.08° N, 113.22° E	C
G-4	Qiqihar (QHR)	47.37° N, 123.92° E	C
(Heilongjiang	Harbin (HRB)	45.75° N, 126.63° E	A
and Jilin Province)	Mudanjiang (MDJ)	44.58° N, 129.60° E	C
	Changchun (CC)	43.92° N, 125.30° E	A
G-5	Fushun (FS)	41.51° N, 123.54° E	C
(Liaoning	Shenyang (SY)	41.80° N, 123.38° E	A
Province)	Anshan (AS)	41.06° N, 123.00° E	C
G-6	Beijing (BeJ)	39.90° N, 116.47° E	A
(Beijing, Tianjin,	Tianjin (TJ)	39.17° N, 117.17° E	A
Hebei Province and Dalian City)	Shijiazhuang (SJZ)	38.05° N, 114.43° E	A
	Qinhuangdao (QHD)	39.90° N, 119.62° E	B
	Dalian (DL)	38.90° N, 121.63° E	B
G-7	Yantai (YT)	37.55° N, 121.33° E	A
(Shandong	Qingdao (QD)	36.07° N, 120.32° E	A
Province and	Rizhao (RZ)	35.23° N, 119.32° E	C
Lianyungang City)	Lianyungang (LYG)	34.59° N, 119.16° E	B
	Weifang (WF)	36.43° N, 119.06° E	C
	Zibo (ZB)	36.48° N, 118.03° E	C
	Jinan (JNa)	36.67° N, 117.03° E	A
	Tai'an (TA)	36.11° N, 117.08° E	C
	Zaozhuang (ZZh)	34.52° N, 117.33° E	C
	Jining (JNi)	35.23° N, 116.33° E	C
G-8	Kaifeng (KF)	34.87° N, 114.38° E	C
(Henan Province)	Zhengzhou (ZhZ)	34.73° N, 113.70° E	A
	Pingdingshan (PDS)	33.44° N, 113.17° E	C

[a] Here API data available period was denoted by A: from June 2000 to February 2007, B: from June 2001 to February 2007, C: from June 2004 to February 2007, and D: from January 2006 to February 2007.

Table 1. Continued.

Group (Representative area)	City	Latitude, Longitude	API data period[a]
G-9	Hefei (HF)	31.85° N, 117.27° E	A
(Shanghai,	Wuhu (WHu)	31.35° N, 118.33° E	C
Anhui,	Nanjing (NJ)	32.05° N, 118.77° E	A
Jiangsu,	Yangzhou (YZ)	32.23° N, 119.26° E	C
and Zhejiang Province)	Zhenjiang (ZheJ)	32.11° N, 119.27° E	C
	Nantong (NT)	32.01° N, 120.51° E	A
	Suzhou (SZ)	31.33° N, 120.65° E	A
	Shanghai (SH)	31.20° N, 121.43° E	A
	Huzhou (HuZ)	30.52° N, 120.06° E	C
	Hangzhou (HaZ)	30.25° N, 120.17° E	A
	Shaoxing (SX)	30.00° N, 120.34° E	C
	Ningbo (NB)	29.88° N, 121.57° E	B
G-10	Jiujiang (JJ)	29.72° N, 115.98° E	C
(Jiangxi, Hubei	Nanchang (NCha)	28.68° N, 115.88° E	A
and Hunan	Wuhan (WHa)	30.62° N, 114.33° E	A
Province)	Jingzhou (JZ)	30.33° N, 112.18° E	C
	Changsha (CS)	28.20° N, 112.92° E	A
	Changde (ChaD)	29.00° N, 111.65° E	C
	Zhangjiajie (ZJJ)	29.08° N, 110.29° E	C
	Nanchong (NCho)	30.49° N, 106.04° E	D
	Chongqing (CQ)	29.55° N, 106.55° E	A
G-11	Luzhou (LuZ)	28.90° N, 105.45° E	C
(Chongqing and	Zigong (ZG)	29.23° N, 104.46° E	D
Sichuan Province)	Chengdu (CheD)	30.65° N, 104.07° E	A
	Deyang (DY)	31.09° N, 104.22° E	C
	Mianyang (MY)	31.30° N, 104.42° E	C
G-12	Qujing (QJ)	25.30° N, 103.48° E	C
(Yunnan Province)	Kunming (KM)	25.05° N, 102.70° E	A
	Yuxi (YX)	24.22° N, 102.32° E	C
G-13	Guiyang (GY)	26.57° N, 106.72° E	A
(Guangxi,	Guilin (GL)	25.30° N, 110.17° E	B
Guizhou,	Liuzhou (LiZ)	24.33° N, 109.32° E	C
Hainan Province	Nanning (NN)	22.78° N, 108.35° E	A
and	Beihai (BH)	21.28° N, 109.07° E	B
Zhanjiang City)	Zhanjiang (ZhaJ)	21.11° N, 110.24° E	A
	Haikou (HK)	20.05° N, 110.17° E	A
G-14	Shaoguan (SG)	24.80° N, 113.55° E	C
(Guangdong, Fujian Province	Guangzhou (GZ)	23.17° N, 113.30° E	A
and Wenzhou Ciy)	Zhuhai (ZH)	22.17° N, 113.34° E	A
	Shenzhen (ShZ)	22.33° N, 114.07° E	A
	Shantou (ST)	23.35° N, 116.67° E	A
	Xiamen (XM)	24.43° N, 118.07° E	A
	Quanzhou (QZ)	24.90° N, 118.62° E	C
	Fuzhou (FZ)	26.03° N, 119.32° E	A
	Wenzhou (WZ)	28.00° N, 120.63° E	A
	Kelamayi (KLY)	45.36° N, 84.51° E	C
	Urumchi (UMQ)	43.77° N, 87.60° E	A
	Lhasa (LS)	29.65° N, 91.03° E	A

[a] Here API data available period was denoted by A: from June 2000 to February 2007, B: from June 2001 to February 2007, C: from June 2004 to February 2007, and D: from January 2006 to February 2007.

Table 2. Air quality classifications corresponding to the air pollution indexes (APIs), air quality management recommendations, and pollutant concentrations in China.

Air pollution index (API)	Air quality classification		Air quality management recommendation	Corresponding daily average pollutant concentration, μg m^{-3}		
				PM_{10}	SO_2	NO_2
API≤50	I	Clean	No action is needed.	PM_{10}≤50	SO_2≤50	NO_2≤80
50<API≤100	II	Good	No action is needed.	50<PM_{10}≤150	50<SO_2≤150	80<NO_2≤120
100<API≤150	III_1	Low-level	Persons should be	150<PM_{10}≤250	150<SO_2≤475	120<NO_2≤190
150<API≤200	III_2	pollution	careful in outdoor activities.	250<PM_{10}≤350	475<SO_2≤800	190<NO_2≤280
200<API≤250	IV_1	Mid-level pollution	Persons with existing heart or respiratory illnesses are advised to reduce physical exertion and outdoor activities.	350<PM_{10}≤385	800<SO_2≤1200	280<NO_2≤422.5
250<API≤300	IV_2			385<PM_{10}≤420	1200<SO_2≤1600	422.5<NO_2≤565
300<API≤500	V	High-level pollution	Air pollution is severe; The general public is advised to reduce physical exertion and outdoor activities.	420<PM_{10}≤600	1600<SO_2≤2600	565<NO_2≤940

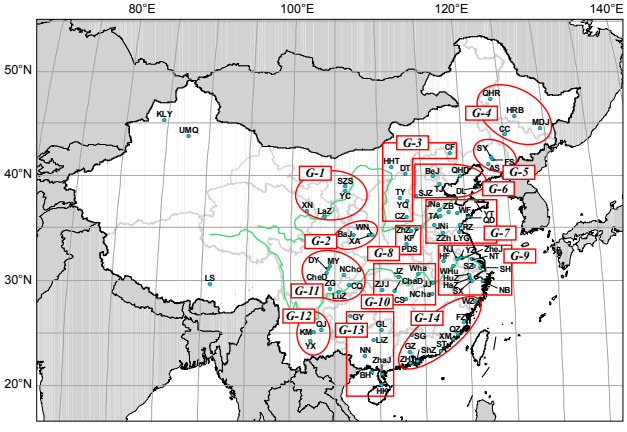

Fig. 1. Locations of the eighty-six Chinese cities for which data are available. Full names of these cities are listed in Table 1. Red frames labeled with G-1 through to G-14 include the cities assigned to the specific group as in Table 1.

2 Data and methods

2.1 Air Pollution Index (API) data

The Chinese air pollution index (API) is a semi-quantitative measure for uniformly reporting air quality, and it is based on a set of atmospheric constituents that have implications for human health. The API for each city, which is reported daily, converts the concentrations of the pollutants of interest into a dimensionless number from 0 to 500. To calculate the APIs, (1) five pollutants (PM_{10}, SO_2, NO_2, CO and O_3) are continuously measured at several monitoring stations in different districts or types of areas in a city (commercial, cultural, downtown, residential, traffic, industrial, etc.) and at a clean background station; (2) the daily average concentrations of these pollutants (except CO and O_3 which are reported as hourly means) are then calculated from the measurements made at all of the stations; (3) a sub-pollution index (sPI) is calculated for each pollutant by linear interpolation of the average concentration of the specific pollutant between the grading limits for each air quality classification listed in Table 2; (4) the maximum sPI is reported as the API for the city and day, and the pollutant with the maximum sPI is reported as the P_{prin}. The APIs thus provide a broad measure of the air quality in the entire city, including polluted areas as well as a clean site. Air quality classifications corresponding to the APIs, air quality management recommendations, and pollutant concentrations are summarized in Table 2. Further information about the API may be found in Zhang et al. (2003), Chu et al. (2008), and from the website of the Ministry of Environmental Protection of the People's Republic of China (http://jcs.mep.gov.cn/hjzl/200604/t20060426_76155.htm).

API records for eight-six major Chinese cities (State Environmental Protection Agency, available at http://www.sepa.gov.cn/quality/air.php3) spanning from June 2000 to February 2007 were used in the present study. Spatial coverage of data is concentrated in mid-eastern China (east of 100° E) (Fig. 1, Table 1). The entire dataset is composed of a total of 150 428 observations: the data for forty-one cities spans ∼7 years (June 2000 to February 2007), six cities cover ∼6 years (June 2001 to February 2007), thirty-seven cities ∼3 years (June 2004 to February 2007), and two cities ∼1 year (January 2006 to February 2007, Table 1).

2.2 PM_{10} Data

For the days when PM_{10} was reported as P_{prin}, daily PM_{10} concentrations were derived from the APIs by using the following equation:

$$C=[(I-I_{\text{low}})/(I_{\text{high}}-I_{\text{low}})]\times(C_{\text{high}}-C_{\text{low}})+C_{\text{low}}, \quad (1)$$

where C is the concentration of PM_{10}, I is the API reported. I_{low} and I_{high} represent API grading limits that are lower and larger than I, respectively; C_{high} and C_{low} denote the PM_{10} concentrations corresponding to I_{high} and I_{low} (Table 2), respectively. The method for calculating PM_{10} concentrations from APIs has been described in detail by Zhang et al. (2003). A total of 137 845 PM_{10} concentrations (on days when PM_{10} was P_{prin} or no P_{prin} was reported) were calculated using this approach, and this accounts for 91.6% of the API records. The other 8.1% and 0.3% of the API records correspond to days when SO_2 or NO_2 was reported as P_{prin}. Characteristics of the deduced PM_{10} concentrations are the main focus of this paper, and the days when the oxides of sulfur or nitrogen were the P_{prin} are not considered further.

In China, PM_{10} concentrations are most often measured with the use of Tapered Element Oscillating Microbalance analyzers (TEOMs, model 1400a, Rupprecht & Patashnick, USA) deployed at the stations by the EPA-China environment monitoring system. The uncertainty of the daily PM_{10} measurement is typically less than 1% (Xia et al., 2006). However, for some cities and stations, β ray particulate monitors (model BAM-1020, Met One, USA) were used to monitor PM_{10}. The principles of the operation of the TEOM analyzers and β ray particulate monitors as well as their field applications are summarized elsewhere (Bari et al., 2003; http://www.metone.com/documents/BAM-1020_6-08.pdf).

It is worth noting that for the days when PM_{10} was P_{prin} and the API was reported as 500, the PM_{10} mass loadings actually could have exceeded the upper limit for the air quality classification of "high-level pollution" ($600\,\mu g\,m^{-3}$). Such high paticulate loading can occur during severe dust storms in some northern cities. However, in this study, we set all of the API records of 500 to PM_{10} loadings of $600\,\mu g\,m^{-3}$. This approximation does introduce some uncertainty in the analysis, but the instances when this happened were infrequent. For the full dataset, only twenty-five cities had maximum API records of API = 500. Furthermore, only four cities recorded more than ten days when API = 500; these were Lanzhou (47 days), Urumchi (36 days), Xining (24 days) and Beijing (12 days), and the days when API = 500 accounted for small percentages, about 1.9%, 1.5%, 0.98% and 0.49%, of the days with API records (2451 days). Taken together, the other twenty-one cities had 57 records with a maximum API (API = 500). Therefore, the impact of this uncertainty should be quite limited.

Another consideration is that no P_{prin} was reported on days when the API was less than 50 (the air quality classified as "clean"). In this regard, an inspection and comparison of the daily sPI records for PM_{10}, SO_2 and NO_2 in selected cities has shown that when no P_{prin} was reported, PM_{10} most often had the highest sPI, and therefore the APIs were most often a reflection of the PM_{10} loadings. Accordingly, for the days when no P_{prin} reported, we assumed that PM_{10} was the P_{prin} that day and deduced PM_{10} concentration according to Eq. (1). This is another source of uncertainty, but again the impact of this assumption is likely to be small.

As the data quality (the validity of this PM_{10} data set) is of the foremost concern, a comparison was conducted between this study and related previous work. The specific concern here is that the use of TEOM–based analyzers (which are commonly used in the EPA-China's air quality monitoring network) can result in underestimation of the aerosol mass because the elevated temperatures of the TEOMs (50 °C) can cause the loss of some material via volatilization. King (2000) has reported that the results obtained with the TEOM–based analyzers are similar to the results of other instruments, but the TEOM results tend to be lower by about 30% because of the volatilization effect. Sciare et al. (2007) has indicated that the mass contributions from semi-volatile material (SVM) and liquid water in Beijing aerosols can cause large errors in TEOM results. These authors showed losses of SVM as high as $140\,\mu g\,m^{-3}$ during high relative humidity (RH, >60%) periods in summer 2004.

It is worth noting that the error of TEOM measurements (heating at 50 °C) due to volatilization of SVM is systematic in the sense that it is always negative. This potential artifact in PM mass measurements could therefore result in a systematic underestimation of PM_{10}. On the other hand, literature reported PM_{10} mass concentrations based on filter sampling and gravimetry are subject to both positive and negative artifacts. That is, reactive gases can accumulate on the filters, but there also can be losses of SVM – such as nitrate and some organic material – via volatilization (Turpin et al., 2000).

These comparisons show that any artifacts in the PM_{10} dataset would likely have a limited influence on the characteristics of spatial distribution and temporal variations in PM_{10} as revealed here. That is, the PM_{10} values calculated from the APIs were generally comparable with the aerosol concentrations based on other techniques such as filter sampling and gravimetry (supplementary material 1). Linear regression (Fig. 2) shows that the literature reported PM_{10} concentrations were about 10% higher than our API-deduced PM_{10}, and the correlation coefficient was 0.84 ($p<0.0001$ significance), thus validating the API-derived PM_{10} concentrations in our study. Furthermore, because of differences in site selection – as noted above, a clean background site is included in the stations used to calculate APIs – it is possible that the literature reported aerosol concentrations, which mostly measured at residential, commercial or heavily trafficked site, were in fact higher than the API-deduced PM_{10} values.

Other researchers (Okuda et al., 2004, 2008; Bi et al., 2007) have compared PM estimated from API records and measured PM, and they found similar results confirming the validity of the API dataset. For example, studies have shown that the monthly mean PM_{10} concentrations reported by EPA-China in Nanning city during 2006 were close to those from a network operated by the China Meteorological Administration, and they showed the same variations with

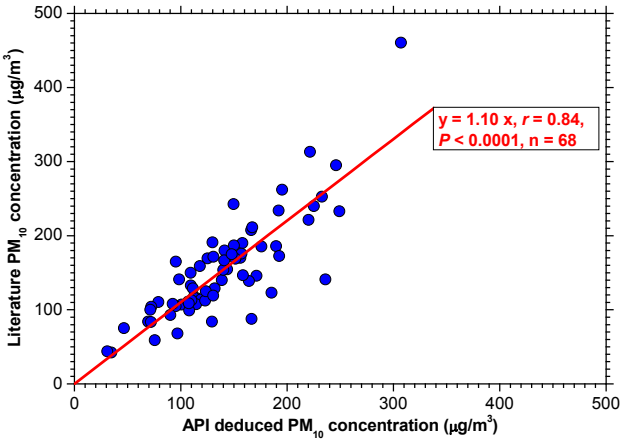

Fig. 2. Linear correlation between the API-deduced PM_{10} concentrations and the literature reported PM_{10} concentrations. The data used in this analysis are adapted from those shown in the Supplementary material 1 – Validation of the API deduced PM_{10} data.

time (Mo et al., 2008). These comparisons all attest to the validity of the API-based PM_{10} data used in our study.

2.3 Grouping the cities according to APIs

A fuzzy clustering procedure was used to determine the similarities between the APIs of the cities (supplementary material 2). In addition, the relationships between among the APIs and the geographical locations of these cities were taken into account in the grouping procedure. For example, the cities in a specific topographical basin were mostly assigned to a same group; thus, Huhehot and Datong which are both located on the northeastern margin of the Great Bend of the Yellow River were assigned to group G-3. On the other hand, cities located on different sides of a mountain were assigned to different groups, e.g. Shijiazhuang and Taiyuan which are located on the eastern and the western sides of the Taihang Mountains are assigned to groups G-6 and G-3, respectively. Meanwhile, cities in the same administrative prefecture (province) and those adjacent geographically were in most cases assigned to the same group for the convenience of discussion.

Through these procedures, eighty-three cities in mid-eastern China (longitude 100° E to 130° E) are divided into fourteen groups (Fig. 1, Table 1). These groups generally correspond to provincial regions. Three cities, Kelamayi (KLY), Urumchi (UMQ) and Lhasa (LS) located in western China were not included in these groups. To better understand spatial patterns in the air quality categories, the fourteen groups of the cities (Fig. 1, Table 1) were further partitioned into northern, middle and southern zones, with the Qinlin Mountain – the Huaihe River and the Yunnan-Guizhou Plateau – the Jiangnan Hill – the Wuyi Mountain as boundaries between zones (marked with black dash lines, Fig. 3).

The northern zone (north of 33 °N, including thirty-eight cities, i.e. G-1 to G-8) extended westward to the northeastern margin of the Tibetan Plateau, northward to the Chinese boundary with Mongolia and Russia, eastward to the Japan Sea, the Bohai sea and the Yellow sea. The middle zone (between 28° N to 33° N, including twenty-six cities, i.e. G-9 to G-11) extended westward to the eastern margin of the Tibetan Plateau, eastward to the Yellow sea and the East China Sea. While the southern zone (south of 28° N, including nineteen cities, i.e. G-12 to G-14) extended westward to the southeastern margin of the Tibetan Plateau, eastward to the East China Sea and Taiwan Island, and southward to the South China Sea. The northern and middle zones actually contain two basins oriented east/west while the southern zone is mainly a hilly area near the South China Sea and the East China Sea.

3 Results and discussion

An inspection of the Chinese API records suggests that PM_{10} pollution is likely a greater concern than SO_2 and NO_2 in major cities because PM_{10} is the most common P_{prin} (Table 3). One can see that for the northern and middle zones of the country, PM_{10} was P_{prin} on more than 80% of the days; while for the southern zone, about half of the days had PM_{10} as P_{prin} (and ∼40% of the days with no P_{prin} reported). The percentages of days with SO_2 as P_{prin} ranged from 6.6% to 9.3% for the three latitudinal zones. In comparison, the numbers of days with NO_2 as P_{prin} were quite small but with relatively larger proportions for the southern zone (0.87%) compared with the northern and the southern zones (0.11% and 0.12%, respectively). This pattern in NO_2 as P_{prin} is probably due to more emissions from motor vehicle and more favorable conditions for the photochemical production of NO_2 in the south.

3.1 Occurrences of the air quality categories

The percent occurrences of days with an air quality category of "clean" (API≤50) were greater than 17.4% for most of the cities in the southern zone (hereinafter referred to as the southern cities) but less than that for most of the middle and northern cities (Fig. 3a). Another feature of the data, which was to be expected, was that the occurrences of "clean" air quality were generally greater for the coastal cities compared with the inland cities (Fig. 3a). Fig. 3b illustrates the percent occurrences of the days with air quality classification as "clean" or "good" (API≤100, that is, days on which the air quality met the Chinese National Grade II Ambient Air Quality Standard, CNAAQS-GII). One can see that in the southern zone, fifteen cities had air quality that met this standard on more than 95% of the days. The exceptions to this were

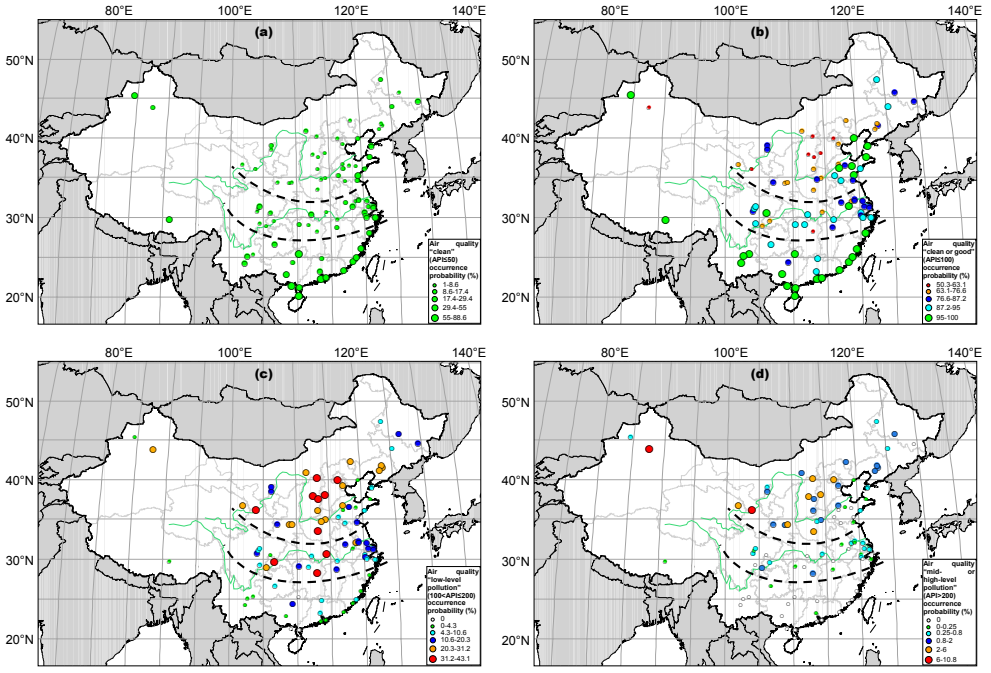

Fig. 3. Spatial distribution of the occurrence probability of the days with air quality classification as **(a)** "clean (API ≤50)", **(b)** "clean or good (API≤100)", **(c)** "low-level pollution (100<API≤200)" and **(d)** "mid- or high-level pollution (API >200)" for the eighty-six cities.

Guiyang, Liuzhou, Shaoguan and Guangzhou; in these four cities, less than 95%, but more than 76.6%, of the days had air quality that met the standard.

Meanwhile in the northern zone, there were only six cities (four coastal cities: Dalian, Qinhuangdao, Yantai, Rizhao and two inland cities: Tai'an, Weifang) that had more than 95% of the days when the air quality met CNAAQS-GII (Fig. 3b). The cities that most often met the standard (occurrences of "clean" or "good" air quality >76.6%, Fig. 3b) were restricted to the coastal area (six cities), the Shandong Peninsula (SDP, five inland cities), and the remote Heilongjiang and Jilin Provinces (three and one cities, respectively). In the remaining large area of the northern zone, eighteen of the twenty-three cities, less than 76.6% (but more than 50.3%) of the days had air quality that met the standard (Fig. 3b).

For the cities in the middle zone, the percentages of the days on which air quality met CNAAQS-GII were intermediate between the northern and the southern zones (Fig. 3b). In contrast to the coastal cities in the other two zones, the occurrences of "clean" or "good" air quality for the coastal cities in the middle zone were less than 95% (Fig. 3b). This was most likely due to heavy anthropogenic emissions in YRD, which is on the coast of the middle zone.

The percent occurrences of days with air quality categorized as "low-level pollution" (100<API≤200) were larger for the northern cities than for those in the middle zone; and the probabilities for this classification were lowest for the cities in the southern zone (less than 10.6% except Liuzhou, Fig. 3c). Similar patterns can be seen for the occurrences of days with air quality categories of "mid- or high-level pollution" (API >200, Fig. 3d). Except for Guiyang and Guangzhou, which had relatively low occurrences of "mid- or high-level pollution" (0.041% and 0.12%, respectively), these classifications never occurred in the southern zone.

3.2 Seasonal variations of the APIs and PM_{10}

High APIs most often occur during winter (December, January and February) and spring (March, April and May) while the lowest APIs are recorded during summer (June, July and August, Fig. 4). This is true for the individual cities and more generally for the three zones. The seasonality in PM_{10} for the three latitudinal zones was similar to that of the APIs, i.e. with wintertime maxima and summertime minima (Table 4). In addition, the seasonal variability of PM_{10} in the southern zone was not as large as in the other zones.

The wintertime PM_{10} maxima were associated with the combustion of fossil fuels for domestic heating (Li et al., 2008) and with more frequent occurrences of stagnant weather and intensive temperature inversion during the colder months. These can result in the accumulation of atmospheric particles and lead to high PM episodes (He et al., 2001; Xia, et al., 2006; Chan and Yao, 2008). Meanwhile, high springtime PM_{10} concentrations always followed the wintertime PM_{10} maxima (Table 4), and this is probably due to dust events (Wang et al., 2004b). The exception

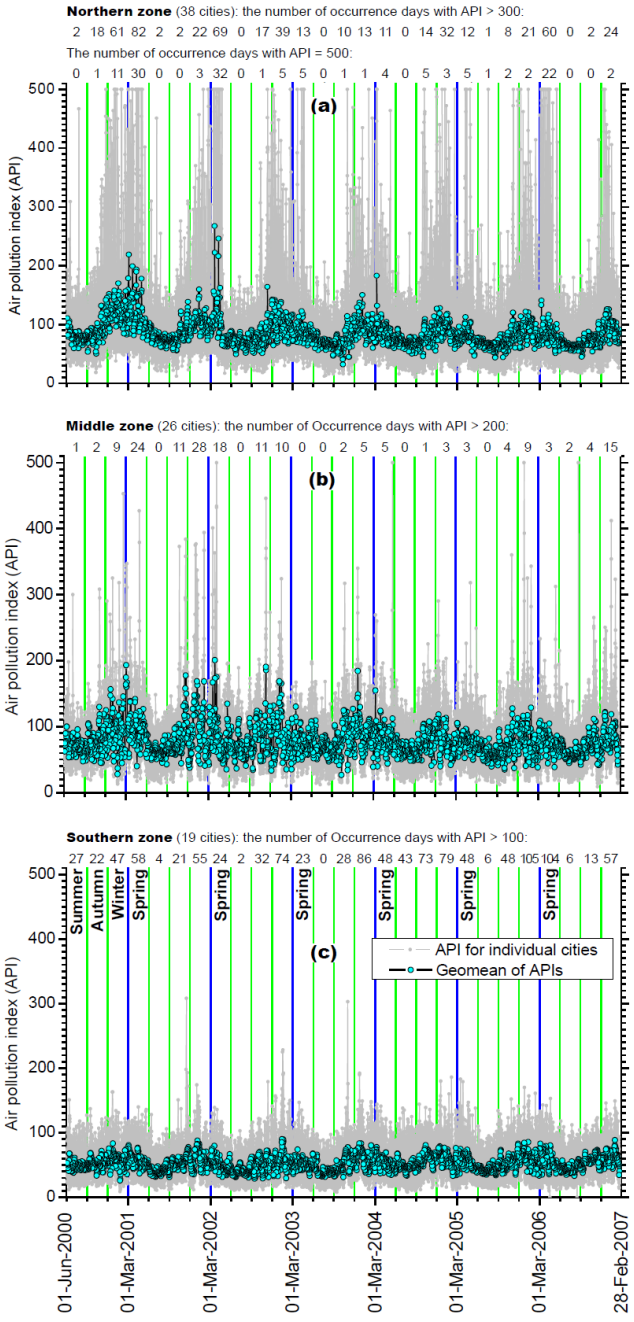

Fig. 4. Variations of the daily air pollution indexes (APIs) for the **(a)** northern, **(b)** middle, and **(c)** southern latitudinal zones. Light gray dots linked with light gray straight solid lines denote the daily APIs for the individual cities, while cyan dots linked with black straight solid lines donate the daily geometric mean APIs for the three latitudinal zones. The numbers of occurrence days with high APIs for the cities in the three latitudinal zones are also presented at the top of (a), (b) and (c).

is slightly lower PM_{10} levels in spring than autumn in the southern zone where the influence from dust events is weakest. In contrast, compared with other seasons, the PM_{10} minima in summer were typically associated with (1) the absence of anthropogenic emissions from domestic heating, (2) more efficient diffusion-dilution of the pollutants due to enhanced convection in a higher atmospheric mixing layer (Xia, et al., 2006), (3) more frequent and abundant precipitation due to the summer monsoon which increases wet scavenging and (4) the inflow of comparatively clean maritime air in the summertime prevailing wind pattern, especially in coastal areas.

For the cities in the northern zone, the maximum APIs were commonly 500 during winter and spring (Fig. 4a), but they rarely (four records) reached 500 for the cities in the middle zone (Fig. 4b). Continuing this trend, the maximum APIs for cities in the southern zone only reached 300 for a few days in autumn 2001 and 2003 (Fig. 4c). A possible explanation for this is that strong wintertime emissions from heating as well as mineral aerosol from springtime dust storms impact the northern zone, and variations in sources such as these can undoubtedly lead to strong seasonal changes in the APIs. In comparison, in southern China, there is less domestic heating in winter, and there are weaker influences of dust storms in spring.

Table 3. Proportions of days with PM_{10}, SO_2 and NO_2 as the principal pollutant in the full set of air pollution index (API) records for the fourteen groups and three latitudinal zones.

Group/Zone (City)	Proportions of days as principal pollutant[a]			
	None (API≤50)	PM_{10}	SO_2	NO_2
G-1	5.6	85.8	8.5	0.036
G-2	1.9	96.0	2.0	
G-3	6.7	78.5	14.2	0.68
G-4	9.7	89.7	0.5	0.12
G-5	2.1	91.7	6.3	
G-6	9.1	76.5	14.4	
G-7	14.4	77.8	7.8	
G-8	3.5	92.7	3.8	0.045
Northern Zone[b]	8.3	83.2	8.4	0.11
G-9	17.4	81.2	1.2	0.22
G-10	8.6	81.6	9.9	
G-11	7.9	76.1	16.0	0.011
Middle Zone	13.0	80.2	6.6	0.12
G-12	15.8	68.4	15.8	
G-13	53.3	32.1	14.6	
G-14	36.3	58.3	3.6	1.8
Southern Zone	40.6	49.3	9.3	0.87
Kelamayi	45.5	54.5		
Urumchi	15.2	69.4	15.4	0.041
Lhasa	40.8	59.2		

[a] Proportion in percentage (%).
[b] The three latitudinal zones are same as those illustrated in Fig. 3.

Table 4. Seasonal arithmetic mean PM_{10} concentrations for the fourteen groups and three latitudinal zones.

	Arithmetic mean ± Standard deviation[a] (n[b])				
Group/Zone (City)	Whole study period	Spring	Summer	Autumn	Winter
G-1	139.3±75.3 (2451)	164.8±98.6 (552)	94.5±28.4 (640)	119.0±48.7 (637)	183.4±73.8 (622)
G-2	143.3±63.5 (2451)	142.9±69.4 (552)	113.6±36.0 (640)	136.4±56.5 (637)	181.1±68.3 (622)
G-3	146.7±73.2 (2430)	149.2±80.5 (551)	111.1±38.9 (640)	136.7±61.8 (635)	192.5±80.7 (604)
G-4	104.4±47.5 (2451)	108.5±53.7 (552)	74.7±20.2 (640)	95.5±33.2 (637)	140.3±50.1 (622)
G-5	144.7±66.2 (2425)	157.6±76.1 (552)	113.5±35.0 (640)	127.3±47.4 (626)	183.7±74.9 (607)
G-6	125.1±62.9 (2414)	140.4±70.3 (551)	98.5±34.4 (640)	116.0±56.3 (636)	149.4±72.6 (587)
G-7	96.6±39.1 (2444)	109.6±45.8 (552)	76.3±21.9 (640)	88.8±30.9 (637)	114.3±41.8 (615)
G-8	124.8±55.6 (2432)	132.0±55.3 (551)	101.8±34.3 (639)	123.1±57.1 (636)	144.3±63.1 (606)
Northern Zone[c]	117.9±41.0 (2451)	127.9±44.4 (552)	90.3±17.9 (640)	107.9±32.8 (637)	147.8±39.9 (622)
G-9	98.9±47.6 (2451)	110.4±51.1 (552)	78.0±28.4 (640)	99.3±46.7 (637)	109.9±53.6 (622)
G-10	116.6±55.1 (2449)	118.4±50.5 (552)	86.6±29.9 (640)	123.4±53.2 (637)	139.1±66.5 (620)
G-11	118.0±46.8 (2451)	128.0±48.9 (552)	98.3±33.7 (640)	107.9±41.4 (637)	139.7±50.3 (622)
Middle Zone	104.1±43.0 (2451)	112.8±42.9 (552)	81.5±22.7 (640)	104.3±41.0 (637)	119.5±50.7 (622)
G-12	74.9±28.1 (2106)	81.4±29.2 (498)	61.5±21.4 (520)	73.6±27.3 (581)	83.7±28.6 (506)
G-13	49.9±14.5 (2451)	48.8±12.7 (552)	40.9±10.5 (640)	53.9±14.0 (637)	55.9±15.4 (622)
G-14	63.4±24.0 (2451)	66.5±24.0 (552)	47.5±13.0 (640)	66.7±22.0 (637)	73.4±26.8 (622)
Southern Zone	58.2±17.7 (2451)	59.8±16.6 (552)	45.4±9.5 (640)	61.6±16.3 (637)	66.5±19.4 (622)
Kelamayi	57.5±39.9 (990)	53.5±25.0 (183)	57.8±17.5 (273)	68.7±64.9 (273)	48.4±25.8 (261)
Urumchi	156.2±134.5 (2073)	123.9±102.1 (428)	73.9±40.9 (640)	141.8±101.8 (575)	329.9±137.8 (430)
Lhasa	64.7±37.1 (2451)	78.4±36.2 (552)	41.5±19.6 (640)	59.5±28.7 (637)	81.9±44.6 (622)

[a] Concentrations in micrograms per cubic meter calculated from daily geometric mean PM_{10} for the group/zone.
[b] Here n stands for the number of daily geometric mean PM_{10} concentrations for the group/zone.
[c]The three latitudinal zones are same as those illustrated in Fig. 3.

Changes in types of pollutants emitted over decadal timescales could impact the seasonality of air pollution. For example, Guinot et al. (2007) found that the winter "heating season" pollution appears to be of lesser importance in Beijing than previously, whereas automobile traffic is likely to dominate downtown anthropogenic emissions in the future. In addition, problems associated with photochemical processes and the formation of fine secondary particles also tend to occur in Beijing summer when temperatures and relative humidities are high (Song et al., 2002). However, the air pollution situations are complicated as they vary largely between different cities.

Accompanied with the implementation of the air quality improvement measures (such as substituting natural gas for coal, controlling emissions from coal combustion—improving combustion technology and gas desulfurization technology, etc.) in China, a dramatic increase in the number of motor vehicles has occurred at the same time. More stringent standards (such as the Euro-III standards since 2006 in Beijing and the Euro-II standards since 2003 in Shanghai) were also adopted to reduce vehicular emissions of air pollutants (Chan and Yao, 2008). In their review, Chan and Yao (2008) indicated that due to effective control measures, NO_2 and CO concentrations have not increased in China's mega cities (including Beijing, Shanghai as well as Guangzhou, Shenzhen and Hong Kong in PRD) although the number of vehicles has increased by about 10% per year; SO_2 emissions were successfully controlled in Beijing, but not in Shanghai or the PRD; meanwhile, PM pollution is still severe and is the major air pollution problem in the mega cities.

3.3 Influence of Asian Dust on the APIs during Spring

The number of springtime occurrences of the maximum API (= 500) for the northern cities was about 30 for 2001 and 2002; this decreased to about 5 for 2003 through 2005, but increased steeply again to 22 in spring 2006 (top of Fig. 4a). Note that the occurrences as tabulated here reflect the total number of days with API = 500 for all cities in the northern zone, that is, if the API records reached 500 for more than one (e.g. *n*) city on a given day, the number of occurrences was tabulated as *n* for that day. The trend in the numbers of the days with API>300 for the northern cities during spring were similar to the occurrences of the API maxima, from 82 and 69 in 2001 and 2002, respectively, to about 12 for 2003

through 2005, then increasing again to 60 in spring 2006 (top of Fig. 4a).

The high APIs for the northern cities co-varied with the occurrences of dust events, and this reflects the fact that the springtime air quality in northern China can be degraded by Asian dust storms. The dust data used for this comparison are the frequencies of springtime dust storms in northern China that were extracted from satellite images by Zhang et al. (2008). Their study showed that there were 11, 8, 2, 3, 3 and 10 dust events in sequence from 2001 to 2006; and this measure of dust storm activity matches the interannual trend in the occurrence of the maximum APIs for the northern cities during spring (top of Fig. 4a). Li et al. (2007) also reported similar trends in the frequencies of springtime dust events in Shijiazhuang city (2, 0, 1, 2 and 3, respectively for 2002 to 2006). A similar pattern in dust event frequencies also has been reported for Xi'an (Ning et al., 2005). More to the point, Wang et al. (2006) showed that dust events contributed to variations in PM_{10} over fourteen northern cities in China.

3.4 Spatial distribution of PM_{10} versus emissions and precipitation

3.4.1 Spatial distribution of PM_{10}

Figure 5a illustrates the spatial distribution of PM_{10} for the eighty-six individual cities. High PM_{10} (presented as the arithmetic mean in $\mu g\,m^{-3}$) regions in northern China (127 to 192) include Urumchi (156) on the southern margin of the Junggar Basin; Lanzhou (192) and Xining (138) on the northeastern side of the Qinghai-Tibetan Plateau; Weinan (152) and Xi'an (144) in the Guanzhong Basin; Taiyuan (179), Datong (162), Yangquan (153) and Changzhi (132) in Shanxi Province in the basins to the west of the Taihang Mountains; Pingdingshan (156, a city with heavy coal industries) and Kaifeng (133) in Henan Province on the western margin of NCP; Beijing (159), Tianjin (140) and Shijiazhuang (168) in the northern part of NCP; Jinan (135) in the eastern part of NCP; and Shenyang (145), Anshan (132) and Fushun (127) in the southeastern part of the Northeast China Plain.

In the middle zone, the high PM_{10} (arithmetic mean in $\mu g\,m^{-3}$) areas (119 to 147 $\mu g\,m^{-3}$) were Chongqing (142), Chengdu (120) and Luzhou (132) in the Sichuan Basin (SCB), Changsha (147) and Wuhan (135) in central China, Nanjing (125) and Hangzhou (119) in YRD.

The PM_{10} levels in the cities in the southern zone were generally lower than those in the northern zone and the middle zone, and there were no areas with arithmetic mean PM_{10} concentration $>109\,\mu g\,m^{-3}$ (Fig. 5a). However, the arithmetic mean PM_{10} concentrations (in $\mu g\,m^{-3}$) exceeded 80 in four cities: Qujing (91), Guiyang (80.1), Guangzhou (85) and Shaoguan (87), and these were much higher than the total average PM_{10} level of $58\,\mu g\,m^{-3}$ for the southern zone.

In general, the PM_{10} hotspots were in cities with dense populations and intensive industrial activities. Moreover, cities located within geographical basins tended to have higher PM_{10} loadings than those outside the basins. Relatively high PM_{10} concentrations were documented in areas such as central-eastern China, NCP, SCB, YRD (Nanjing and Hangzhou), and PRD (Guangzhou and Shaoguan, PM_{10} concentration $>80\,\mu g\,m^{-3}$, Fig. 5a). These regions also have been identified as high AOD/AOT areas by the radiation/optical measurements and satellite observations (Luo et al., 2000, 2001; Li et al., 2003; Wang et al., 2008). At the same time, one should note that during a pollution episode, the aerosol spatial distribution could be quite different from the average conditions as illustrated in Fig. 5a. More information about the relationships between PM_{10} and optical measurements can be found in Sect. 3.7 below.

The spatial distribution of PM_{10} concentration is not presented here as an interpolated contour plot because the dataset is biased toward sites that are generally the most polluted "points" on a regional scale. That is, the cities typically are high-value centers in the field of PM_{10}, with low-value areas interspersed between these high PM_{10} loci. Although these results do not represent the full spatial distribution of the aerosol as evident in satellite observations, they do provide important insights into the spatial distributions of the aerosol and the problems of air pollution based on independent measurements of PM in surface air.

Table 4 tabulates the arithmetic mean PM_{10} concentrations for the fourteen groups described in Section 2.3 above. Note these values tend to be less than the individual PM_{10} levels in mega cities because some cleaner small and satellite cities are included in the groups. From Table 4 one can see that in the northern zone, G-4 (Heilongjiang and Jilin Provinces) and G-7 (SDP) exhibited lower PM_{10} levels compared with other groups during spring, summer and autumn; while during winter, G-1 (Qinghai, Gansu and Ningxia Provinces), G-2 (Shaanxi Province), G-3 (Inner Mongolian and Shanxi Provinces) and G-5 (Liaoning Province) had higher PM_{10} levels than other groups. For the three groups in the middle zone, G-9 (YRD) showed the lowest PM_{10} concentration in all four seasons. In the southern zone, PM_{10} levels were comparable for the three groups. For a more detailed description of the seasonal patterns of PM_{10} spatial distribution, see supplementary material 3.

Although the spatial distribution of PM_{10} is complex, an overall north to south decrease in our API-derived PM_{10} data for the Chinese cities is distinct and can be seen in Fig. 5a; this will be discussed in detail in Sect. 3.5.

3.4.2 Comparison of PM_{10} with emissions and precipitation

Accurate emissions data are scarce for China, and research in this area is complicated by differences in the combustion technologies used throughout the country and the limited

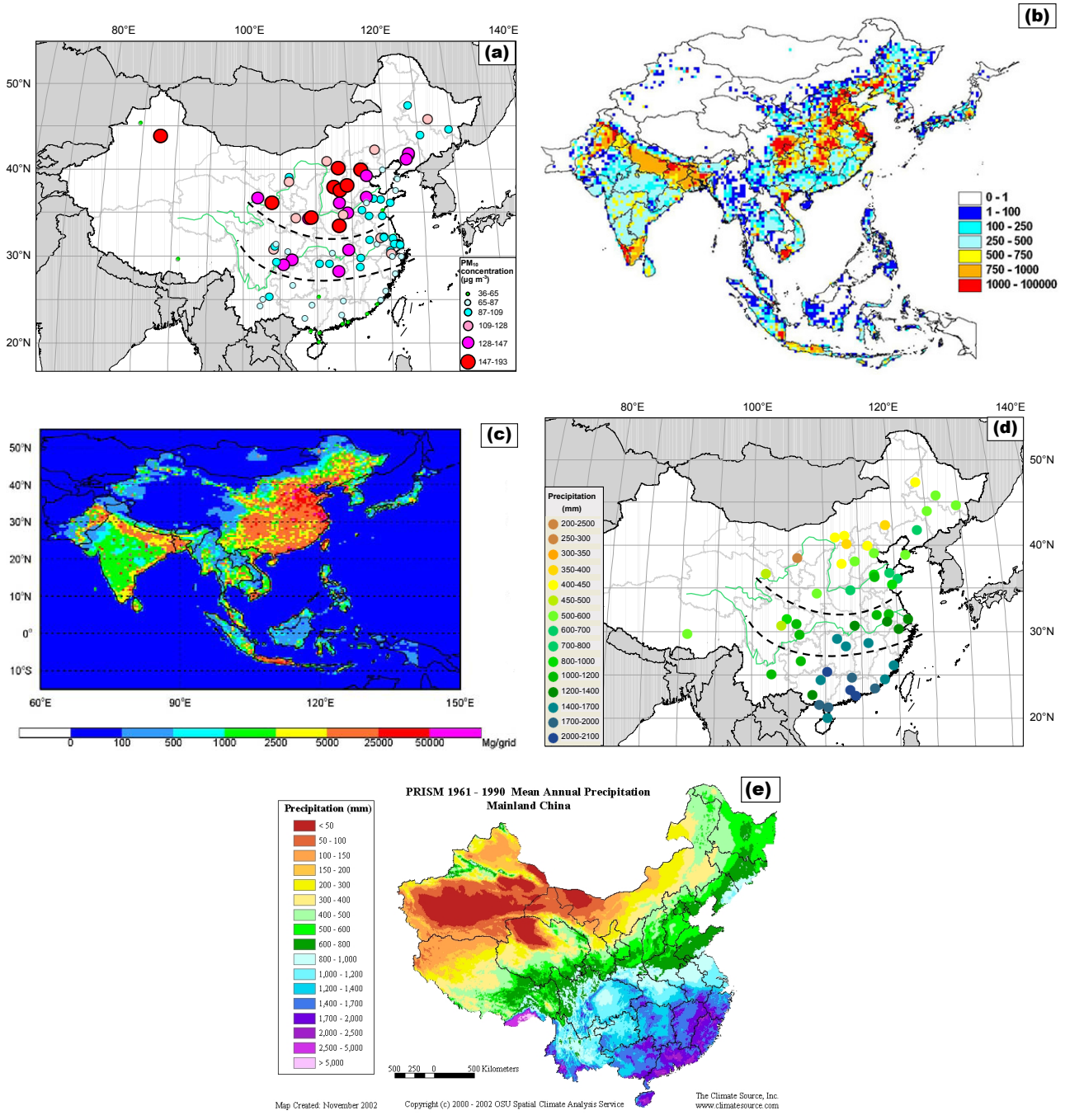

Fig. 5. (a) Spatial distribution of the multi-year (2000 – 2006) average PM_{10} concentrations for the eighty-six Chinese cities; (b) Total Asia emissions of anthropogenic black carbon (BC, units: tonnes/year/0.5°cell) in 2006 (http://www.cgrer.uiowa.edu/EMISSION_DATA_new/index_16.html); **(c)** Emission distributions at 30 min × 30 min resolution of anthropogenic PM_{10} (units: Mg/year per grid) over Asia in 2006 (after Zhang et al., 2009); **(d)** Mean annual precipitation for fifty-one Chinese stations during 2000 – 2006, calculated from the records of these stations extracted from the Global Summary of Day (GSOD) database (ftp://ftp.ncdc.noaa.gov/pub/data/gsod) distributed by the National Climatic Data Center (NCDC), US; **(e)** Mean annual precipitation over mainland China during 1961 – 1990 (The Climate Source, Inc., 2010, http://www.climatesource.com/cn/fact_sheets/chinappt_xl.jpg).

availability of information regarding energy consumption, industrial output, etc. An inventory of anthropogenic air pollutant emissions in Asia was developed for the year 2006 for the INTEX-B project (the Intercontinental Chemical Transport Experiment-Phase B, Zhang et al., 2009). We compare the PM_{10} distributions we derived with the emissions of both BC and PM_{10} from this inventory. Note BC and PM_{10} distributions from this inventory show similar patterns with results from other reseach on the anthropogenic nitric oxide (NO) emissions (see Fig. 7 in Tie et al., 2006b), indicating they are representative of emissions from anthropogenic activities.

PM_{10} loadings in mid-eastern China (Fig. 5a) were generally similar to the emission patterns of anthropogenic BC (Fig. 5b). Cities with high PM_{10} ($>109\,\mu g\,m^{-3}$, indicated by pink-magenta-red symbols with concentrations from low to high, Fig 5a) coincided with the areas with strong BC emissions (>500 tonnes/year/0.5°cell, filled with yellow-orange-red with emissions from less to large, Fig. 5b) such as the Beijing-Tianjin municipalities and southern Hebei Province, mid-eastern Henan Province, and western-central Liaoning Province in northern China. The high PM_{10} area of Chongqing-Chengdu-Luzhou (Fig. 5a) coincided with the intensive BC emission areas of SCB and northwestern Guizhou Province (Fig. 5b), while the high PM_{10} area of Wuhan-Changsha (Fig. 5a) coincided with the intensive BC emission areas of mid-eastern Hubei Province and mid-eastern Hunan Province (Fig. 5b).

In Shanxi Province, on the other hand, the high PM_{10} loadings for Taiyuan-Datong-Yangquan-Changzhi (ranging from 132 to $179\,\mu g\,m^{-3}$, Fig. 5a) were seemingly at odds with the generally moderate BC emissions in that province (Fig. 5b). However, point sources of BC (>500 tonnes/year/0.5°cell, filled with yellow, orange or red) as shown in Fig. 5b coincided quite well with the locations of those four cities in Fig. 5a. The same was true for Weinan, Xi'an and Baoji in Shaanxi Province, for Lanzhou in Gansu Province, for Xining in Qinghai Province, and for Urumchi in the Xinjiang Uyghur Autonomous Region.

In contrast, the distributions of PM_{10} concentration (Fig. 5a) along the east coast of China apparently do not follow BC emissions (Fig. 5b). For example, although BC emissions in SDP and YRD are high (Fig. 5b), the average PM_{10} concentrations for the cities in SDP during 2000 to 2006 were not particularly high, less than $109\,\mu g\,m^{-3}$ except for Jinan ($135\,\mu g\,m^{-3}$, Fig. 5a). PM_{10} concentrations for the cities in YRD also were $<109\,\mu g\,m^{-3}$ except for Nanjing ($125\,\mu g\,m^{-3}$) and Hangzhou ($119\,\mu g\,m^{-3}$, Fig. 5a). Possible reasons for the decoupling of PM_{10} and emissions along the Chinese coast are discussed below.

Emissions of anthropogenic PM_{10} (Fig. 5c) were generally similar to those of BC (Fig. 5b), but the high PM_{10} emission areas are widespread, in contrast to the distributions of strong BC emissions—mostly concentrated in relatively limited regions. Similar to the relationship between the BC emissions and derived PM_{10} described above, the cities with high PM_{10} loadings ($>109\,\mu g\,m^{-3}$, Fig 5a) coincided with the areas with strong PM_{10} emissions (>5000 Mg/year per grid, filled with orange-red-magenta with emissions from less to large, Fig. 5c). This was true for the Beijing-Tianjin municipalities, Hebei-Shanxi-Henan provinces, Hubei-Hunan provinces, and SCB-Guizhou Province.

Along the Chinese coast, including SDP, YRD and PRD, the relatively low PM_{10} loadings (Fig. 5a) were in contrast to the strong PM_{10} emissions there (Fig. 5c). For example, except for Tianjin, the cities along the coast including those around the Bohai Bay and SDP, in YRD and PRD all showed PM_{10} concentrations less than $109\,\mu g\,m^{-3}$ (Fig. 5a). Thus, the intensive PM_{10} emissions in coastal regions bordering the Bohai Sea, the Yellow Sea, the East China Sea, and the South China Sea (Fig. 5c) evidently do not result in especially high PM_{10} loadings.

The discrepancy between the concentrations and emissions of PM_{10} along the coast can be explained by dilution of the pollutants by clean marine air and by wet scavenging of the PM by the more abundant precipitation there. With reference to the latter, an examination of the mean annual precipitaiton for fifty-one Chinese stations from 2000 to 2006 (Fig. 5d) shows that precipitation at the coastal sites is generally larger than those for the inland sites at the same latitude. Long-term averaged annual precipitations (1961 to 1990) for the areas along the Chinese coast were also larger than those for the inland regions at the same latitude (Fig. 5e). These findings support the idea that more PM is scavenged from the atmosphere by precipitation in coastal regions.

Moreover, as RH and liquid water content are related to the levels of SVM and nitrate in aerosols, they are believed to play a major role in the gas-particle partitioning of semi-volatile species; volatilization loss of these SVM can result in underestimation of PM mass by the TEOM measurement heating at 50°C (Sciare et al., 2007). Therefore, the PM_{10} concentrations calculated from APIs may be more strongly affected by this artifact in the costal areas where RH is generally higher compared with inland sites. This may cause artificially lower PM_{10} concentrations within our dataset along the coast.

In summary, except for the coastal areas, the distribution of PM_{10} concentration was generally consistent with the anthropogenic emissions of BC and PM_{10} over China. Additional information about anthropogenic emissions over China with respect to monthly and seasonal variations can be found in supplementary material 4—Monthly mean tropospheric NO_2 over Southeast Asia during October 2004 to February 2007 extracted from OMI (the Ozone Monitoring Instrument) version 1.0 (website, http://www.temis.nl/airpollution/no2col/no2regioomimonth_col3.php) (Boersma, et al., 2007).

3.5 Latitudinal and longitudinal gradients of PM_{10}

The PM_{10} concentrations for the northern zone generally were slightly higher than or comparable with those in the

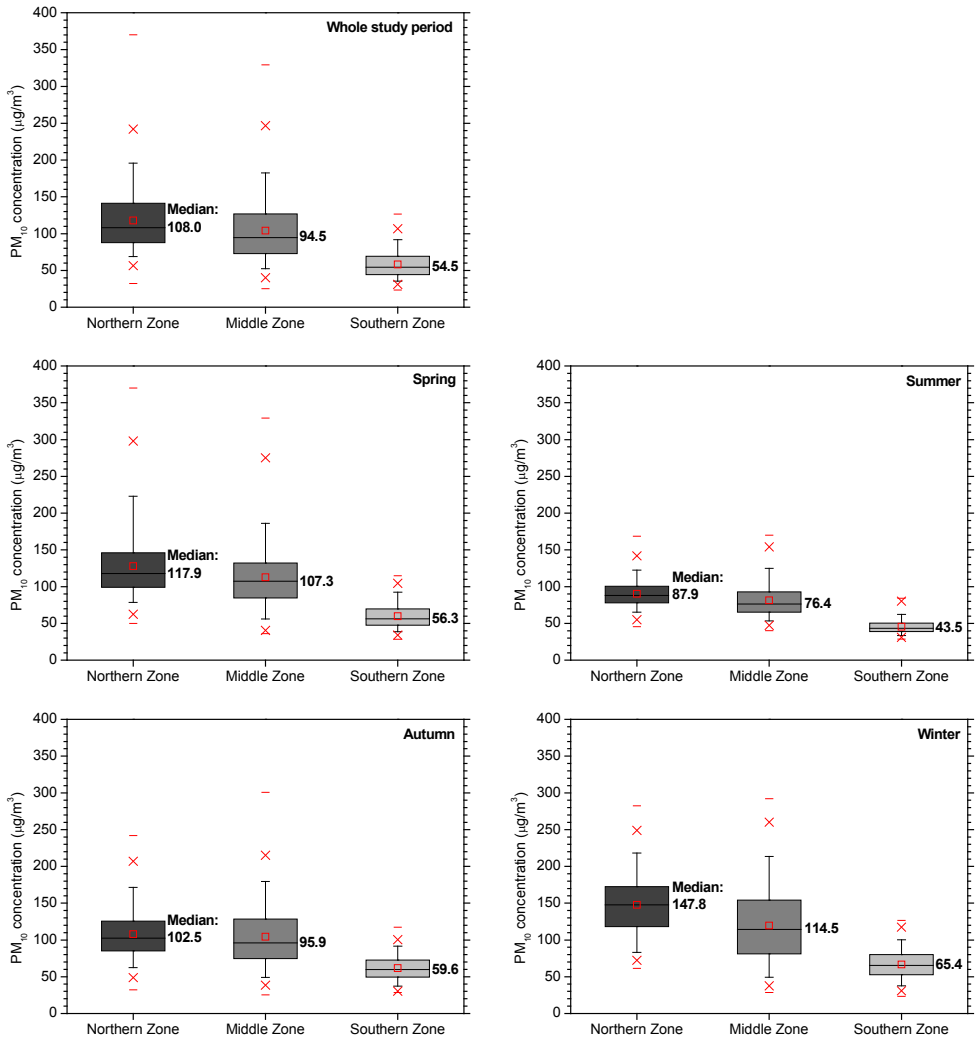

Fig. 6. Comparison of PM_{10} levels and variations for the three latitudinal zones in different seasons: the box-and-stem plots depict the minimum, the 1th, 5th, 25th, 50th (median), 75th, 95th, 99th percentile and the maximum for the PM_{10} concentration, the red square in the box depicts the arithmetic mean PM_{10} concentration, the median PM_{10} concentrations are also presented.

middle zone during spring, summer and autumn (Table 4). In the winter, however, PM_{10} concentrations in the northern zone were much higher than in the other zones, presumably due to emissions from domestic heating in the colder northern zone coupled with the accumulation of pollutants in the stable lower boundary layer (especially during nighttime). Along these lines, the median PM_{10} concentration at Urumchi during winter was 317 $\mu g\,m^{-3}$, which is about three times that in spring and autumn (92 $\mu g\,m^{-3}$ and 116 $\mu g\,m^{-3}$, respectively), and more than five times that in summer (60 $\mu g\,m^{-3}$). This high aerosol loading at Urumchi indicates very severe wintertime PM pollution in that city.

Overall, the PM_{10} concentrations in the southern zone were generally the lowest of the three zones (Table 4); they were only about half of those for the northern zone but more than half of those for the middle zone during all seasons. Although the PM_{10} concentrations showed a north-south difference in all the seasons, it was most pronounced in winter and less so in autumn (Table 4).

In addition to the distinct north to south decrease in PM_{10}, further information on the patterns in PM_{10} can be seen in the box and stem plots shown in Fig. 6; that is, both the concentration and the variability in PM_{10} were the lowest in the southern zone. The PM_{10} variances in the northern zone were greater than the middle zone during spring, comparable during summer, but lower during autumn and winter. Another general feature of the data is that the arithmetic mean PM_{10} concentrations are typically larger than the medians, especially for the northern zone and the middle zone (Fig. 6); this indicates that the PM_{10} concentrations in those parts of the country were periodically elevated by severe pollution episodes.

Possible reasons for the relationship between latitude and PM_{10} loading include (1) greater emissions from domestic heating during winter in the north (see supplementary material 4), (2) stronger impacts from dust storms during spring for the cities in northern China, and (3) more efficient dilution of pollutants by the influx of clean maritime air and more efficient wet scavenging of PM by precipitation in southern China (Fig. 5d and e). In summary, the patterns in PM_{10} reflect the combined impacts of emissions, transport, dilution and removal on aerosol loadings over a broad region.

In addition to the latitudinal gradient, a distinct longitudinal aerosol gradient is evident in the northern zone where PM_{10} concentrations decreased from west to east (supplementary material 5). Weaker influences from desert dust as well as more efficient dilution with relatively clean marine air likely contribute to the low PM_{10} levels in the eastern cities in northern China. A strong west-to-east gradient of BC between 30° N and 35° N also has been observed over the central Pacific Ocean (Kaneyasu and Murayama, 2000). On the other hand, for the cities in the middle and southern zones, PM_{10} concentrations also generally exhibited a decreasing trend from west to east, but the longitudinal differences in those cases were smaller and insignificant.

The latitudinal and longitudinal gradients in PM_{10} concentration as depicted here only show broad patterns in the urban aerosol over China; the spatial distribution of the atmospheric aerosol (as described in Sect. 3.4) is undoubtedly more complicated.

3.6 Temporal trends in urban PM_{10}

3.6.1 Interannual variations

There were changes in the number of cities included in the dataset over the course of the study (Table 1), and to circumvent any biases from this, only the cities with full records (sixteen, eleven, and twelve cities in the northern, middle and southern zone, respectively) were considered in the following assessment of temporal trends in PM_{10} (Fig. 7). A comparison between the entire dataset (all eighty-three cities in the three latitudinal zones) and the subset (thirty-nine cities with full records) shows similar patterns in PM_{10} variations, but the arithmetic means (or medians) of the subset were generally higher.

We used the median values to assess interannual variations in the PM_{10} concentrations for the three latitudinal zones for 2000 to 2006 (Fig. 7). This was done to reduce the influence of the rare exceptionally high values on the results. As noted above, whenever the reported API was 500, the PM_{10} concentration was arbitrarily set to 600. This would have introduced some additional complications into the assessment if it had been based on the arithmetic or geometric mean PM_{10} concentration, but it does not influence the assessments of trends based on the median PM_{10} concentrations as presented here.

For the northern zone, the springtime PM_{10} level decreased from 157 $\mu g\,m^{-3}$ in 2001 to 123 $\mu g\,m^{-3}$ in 2002, and then fluctuated around 120 $\mu g\,m^{-3}$ from 2002 to 2006, with a minimum (108 $\mu g\,m^{-3}$) in spring 2005 (Fig. 7a). The summertime PM_{10} level increased from 2000 to 2001, then decreased from 108 $\mu g\,m^{-3}$ in 2001 to 83 $\mu g\,m^{-3}$ in 2006 (Fig. 7b); the autumn PM_{10} level decreased steadily from 121 $\mu g\,m^{-3}$ in 2000 to 94 $\mu g\,m^{-3}$ in 2004, but then increased to about 100 $\mu g\,m^{-3}$ during 2005–2006 (Fig. 7c). The wintertime PM_{10} level in the northern cities decreased from 189 $\mu g\,m^{-3}$ in 2000 to 136 $\mu g\,m^{-3}$ in 2006, although with a few fluctuations (Fig. 7d). The annual PM_{10} level in the north (125 $\mu g\,m^{-3}$ in 2000) increased at first, then decreased from 136 $\mu g\,m^{-3}$ in 2001 to about 101 $\mu g\,m^{-3}$ during 2005–2006 (Fig. 7e). More generally, the median PM_{10} level over the northern cities decreased 23 $\mu g\,m^{-3}$ from 2000 to 2006 (Fig. 7e), and this decreasing trend was statistically significant ($p<0.01$ significance, $r = 0.89$, n = 7).

For the middle zone, the springtime PM_{10} level varied in a manner similar to that seen in the northern zone (Fig. 7a), probably reflecting the widespread influence of dust events. There was an overall decreasing trend of summertime PM_{10} concentration from 88 $\mu g\,m^{-3}$ to 71 $\mu g\,m^{-3}$ over the course of the study, but with higher levels ($\sim$90 $\mu g\,m^{-3}$) from 2002 to 2004 (Fig. 7b); the autumn PM_{10} level increased from 94 $\mu g\,m^{-3}$ in 2000 to 128 $\mu g\,m^{-3}$ in 2002, then decreased to $\sim$108 $\mu g\,m^{-3}$ from 2003 to 2004 and $\sim$94 $\mu g\,m^{-3}$ during 2005 to 2006 (Fig. 7c); the wintertime PM_{10} level fluctuated around 130 $\mu g\,m^{-3}$ from 2000 to 2003, then decreased to a minimum (96 $\mu g\,m^{-3}$) in winter 2005 but increased again to 126 $\mu g\,m^{-3}$ in 2006 (Fig. 7d). The annual PM_{10} level varied around 100 $\mu g\,m^{-3}$, from 99 $\mu g\,m^{-3}$ in 2000 to 97 $\mu g\,m^{-3}$ in 2006 (Fig. 7e). Overall, the PM_{10} level in the middle zone showed no significant change from the start to the end of the study (-1.7 $\mu g\,m^{-3}$, Fig. 7e).

In the southern zone, the springtime PM_{10} level fluctuated slightly with only minor changes (59.4 $\mu g\,m^{-3}$ in 2001 versus 59.3 $\mu g\,m^{-3}$ in 2006, Fig. 7a), suggesting a weaker influence of dust on PM there. The summertime PM_{10} level decreased from 49 $\mu g\,m^{-3}$ in 2000 to about 41 $\mu g\,m^{-3}$ during 2001–2004, then increased to 46 $\mu g\,m^{-3}$ in 2006 (Fig. 7b); the autumn PM_{10} level fluctuated but increased from 53 $\mu g\,m^{-3}$ in 2000 to 65 $\mu g\,m^{-3}$ in 2006 (Fig. 7c); the wintertime PM_{10} level fluctuated between 63 $\mu g\,m^{-3}$ in 2000 to 73 $\mu g\,m^{-3}$ in 2006 (Fig. 7d); the annual PM_{10} level showed a small increase from 53 $\mu g\,m^{-3}$ in 2000 to 59 $\mu g\,m^{-3}$ in 2006 (Fig. 7e). In general, the PM_{10} level in the southern zone fluctuated but showed a slight increase (+6.2 $\mu g\,m^{-3}$) during the study period (Fig. 7e), but this trend did not pass the 95% confidence level test ($p<0.1$ significance, $r = 0.69$, $n = 7$).

As the springtime PM_{10} level is strongly affected by dust events, the data for that season are considered separately to assess how anthropogenic emissions affect PM_{10}. Our analysis of the data for summer, autumn and winter combined

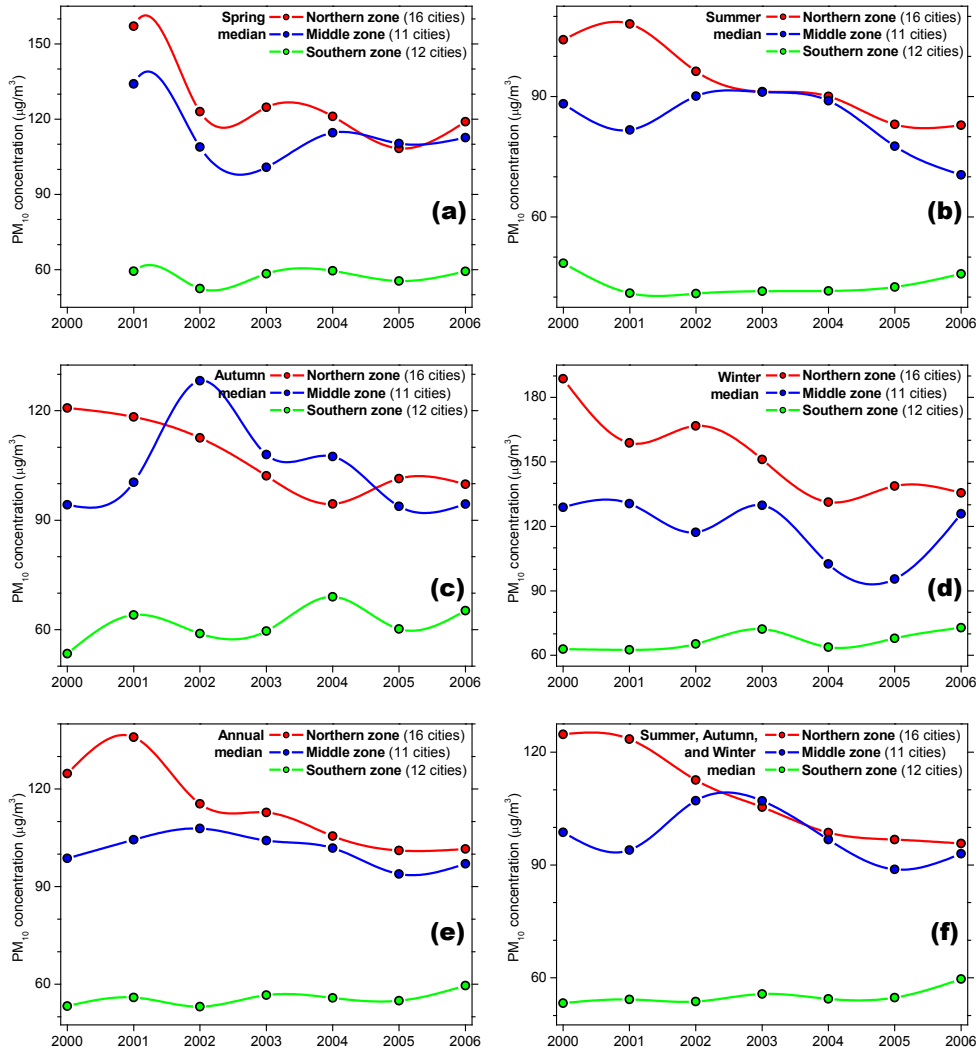

Fig. 7. Interannual variations of the **(a)** spring, **(b)** summer, **(c)** autumn, **(d)** winter, **(e)** annual, and **(f)** summer, autumn and winter combined median PM_{10} concentrations for the three latitudinal zones from 2000 to 2006.

(SAW) showed that the median PM_{10} level in the northern zone decreased from about 124 μg m^{-3} in 2001 and 2002 to about 96 μg m^{-3} in 2005 and 2006 (Fig. 7f). For the middle zone, the SAW PM_{10} level first decreased from 99 μg m^{-3} in 2000 to 94 μg m^{-3} in 2001, then increased to ∼107 μg m^{-3} in 2002 and 2003, but decreased again to a minimum of 89 μg m^{-3} in 2005, and finally increased to 93 μg m^{-3} in 2006 (Fig. 7f). Comparing Fig. 7e with 7f, one can see that for the northern and middle zones, interannual variations in the annual median PM_{10} levels differed from those in the SAW PM_{10} levels, and this was probably due to influence of springtime dust on PM as discussed above. But for the southern zone, the SAW PM_{10} level varied in a manner consistent with that in the annual PM_{10} level (Fig. 7e and f), suggesting little influence from spring dust.

Taken together, in contrast to the small increase of urban PM_{10} concentration in the southern zone (+ 12%), the PM_{10} levels showed a decreasing trend for the northern cities (– 19%) and a negligible decrease for the middle zone (– 1.7%). This may be a result of the country's air pollution control efforts in the urban areas. These efforts include reducing stationary emissions (eliminating some small coal fired power plants, and managing heavy pollution industries), substituting natural gas for coal, controlling mobile source emission from vehicles, improving road conditions, and increasing urban vegetative cover (Duan et al., 2006; Chan and Yao, 2008; Fang et al., 2009).

3.6.2 Evaluation of urban PM_{10} variation trend

Several studies have recently documented a decreasing trend of urban PM_{10} level and a general improvement of urban air

quality in northern and middle China. For example, Chan and Yao (2008) indicated that the annual median PM_{10} concentration in Beijing decreased from 180 $\mu g\,m^{-3}$ in 1999 to 142 $\mu g\,m^{-3}$ in 2005. A study in Lanzhou showed that the concentrations of magnetic minerals in the wintertime urban dustfall samples (collected during 1997–2005) have decreased, indicating an improvement of the winter air quality (Xia et al., 2008). Zhang et al. (2006) also reported that the air quality in Shenyang improved year-by-year from 1995 to 2004. In addition, PM_{10} concentration in Nanchong decreased dramatically from 146 $\mu g\,m^{-3}$ in January 2002–May 2003 (Wen et al., 2004) to 74.6 $\mu g\,m^{-3}$ in January 2006–February 2007. Shi et al. (2008) concluded that the air quality has improved in Shanghai, Nanjing, Hangzhou and Hefei from 2002 to 2005. Moreover, an analysis of data from more than 300 major cities in China indicated that the percentage of cities with PM_{10} concentrations less than 100 $\mu g\,m^{-3}$ increased from 36.8% in 2002 to 62.8% in 2006, and the cities with PM_{10} concentrations greater than 150 $\mu g\,m^{-3}$ decreased from 29.8% to 5.3% (Yao et al., 2009).

It is worth noting that the variation trends in PM_{10} concentration presented here for the three latitude zones in China reflect changes in aerosol loadings in major cities, but they are not necessarily representative of the variations in aerosol concentrations over less populated regions.

We note that coal product usage in China increased from ∼1320 million tons in 2000 to ∼2392 million tons in 2006, and petroleum product usage increased steadily from ∼224 million tons in 2000 to ∼349 million tons in 2006 (source: National Bureau of Statistics China, http://www.stats.gov.cn/tjsj/ndsj/2007/indexch.htm; Fang et al., 2009). On the other hand, technological improvements have been implemented in China, which lead to decrease of the average emission factors of SO_2, NO_χ and $PM_{2.5}$ for coal-fired power plants from 2000 to 2006, especially those for $PM_{2.5}$; meanwhile, the average emission factors of NO_χ, CO and VOC (volatile organic compounds) for gasoline vehicles also decreased significantly from 2000 to 2006 (Zhang et al., 2009). Note emission factor is a representative value that attempts to relate the quantity of a pollutant released to the atmosphere with an activity associated with the release of that pollutant, which is usually expressed as the weight of pollutant divided by a unit weight, volume, distance, or duration of the activity emitting the pollutant (e.g., kilograms of particulate emitted per megagram of coal burned, http://www.epa.gov/ttnchie1/ap42/).

However, according to Streets et al. (2003) and Zhang et al. (2009), except for a decreasing trend in OC (organic carbon) (3.4 Tg→3.2 Tg), China's anthropogenic emissions, including SO_2 (20.4 Tg→31.0 Tg), CO (116 Tg→166.9 Tg) and NMVOC (nonmethane volatile organic compounds, 17.4 Tg→23.2 Tg) increased by about 50% from 2000 to 2006, while those for NO_χ (11.4 Tg→20.8 Tg) and BC (1.05 Tg→1.8 Tg) increased by about 100%. Zhang et al. (2009) estimated 2006 and 2001 emissions for China using a same methodology, and they found that all species show an increasing trend during 2001 to 2006: 36% increase for SO_2, 55% for NO_χ, 18% for CO, 29% for VOC, 13% for PM_{10}, and 14% for $PM_{2.5}$, BC, and OC.

How can the decreasing trend in PM_{10} level from 2000 to 2006 be reconciled with the increases in fossil fuel usage (such as coal and petroleum) and anthropogenic emissions for the country? The most likely explanation is that increasingly stringent emission control standards and air quality management strategies for major cities have led to localized improvements of air quality.

Another possibility is that the sources for the pollution emissions have become more widely dispersed. Along these lines are the effects of growing urbanization. According to Chan and Yao (2008), from 1980 to 2005, the urban population in China increased from 19.6 to 40.5%; the number of cities increased to over 660, and more than 170 cities had over 1 million permanent residents in 2004 (National Bureau of Statistics China, 2005a, 2006a). Meanwhile, mega cities (conventionally defined as cities with populations over 10 000 000) emerged in the 1990s in China and city clusters developed in the proximity of the mega cities (National Bureau of Statistics China, 2005b, 2006b). The economic expansion, especially in rural and under-developed areas of China, has affected the geographical distributions of pollution emissions. This can be seen from the changes in the sources for major air pollutants, including SO_2, NO_x, NMVOC and BC from 2000 to 2006 (see supplementary material 6; Streets et al., 2003; Zhang et al., 2009).

More generally, aerosol loadings vary due to interactions among many processes including emissions (anthropogenic emission and natural dust production), transport (as well as convection influenced dispersion and dilution), photochemical transformation (new particle speciation and production of secondary aerosols), and deposition (dry and wet), with meteorology playing an overarching role. The causes for the variations in aerosol loadings in China are undoubtedly complicated, and results suggesting improvements in air quality in major cities in northern China, while encouraging, should be assessed cautiously; further study is obviously necessary on this issue.

3.7 Comparison of PM_{10} variations with AOD/AOT results

3.7.1 Comparison of PM_{10} with AOD/AOT

As described in Sect. 3.4.1, areas found to have relatively high PM_{10} concentrations such as central-eastern China, NCP, SCB, YRD and PRD (Fig. 5a) also were high AOD/AOT areas as identified by the radiation/optical measurements and satellite observations (Luo et al., 2000, 2001; Li et al., 2003; Wang et al., 2008). Using the AOT data from two AERONET sites (Beijing and Guangzhou, data available from the AERONET web site, http://aeronet.gsfc.nasa.gov/), we conducted a preliminary comparison of the daily AOT

at 440 nm with surface PM_{10} concentration (supplementary material 7). Our comparisons are limited to these two cities because of the limited overlap of the API PM_{10} and AERONET AOT dataset.

The AOTs at 440 nm generally showed good correlations with the surface PM_{10} concentrations at Beijing and Guangzhou. Another important feature of the Beijing data is that the correlation between the AOT at 440 nm and the PM_{10} concentration in summer ($r = 0.63$) is higher than in the other seasons ($r = 0.34$, 0.58 and 0.50 in spring, autumn and winter, respectively). Xia et al. (2006) presented a detailed comparison between AERONET AOT at 440 nm and PM_{10} concentration in Beijing that covered a period of 33 months. Their study also found a higher correlation coefficient in summer ($r = 0.77$) compared with the other seasons ($r = 0.37$, 0.70, and 0.61 in spring, autumn and winter, respectively). They argued that the higher correlation between AOT and PM_{10} in summer indicated that the aerosols are well mixed, and surface measurements then are a good indicator of column-integrated values. These authors attributed the differences in seasonal and diurnal variations between AOT and surface PM_{10} to the variation of atmospheric mixing layer height.

Song et al. (2009) compared three years of MODIS AOD (at 550 nm) with spatial and seasonal variations of PM_{10} concentration for forty-seven sites; they found variability in the relationships between AOD and surface PM_{10} as well as regional differences in their seasonality over China. The correlation coefficients they calculated between PM_{10} and AOD were +0.6 or higher in the southeastern coast but −0.6 or lower in the north-central region; and this regional discrepancy was largely attributed to the difference in the size distributions of aerosols. We discuss in more detail several factors that could cause differences between the surface PM_{10} concentration and the AOD/AOT in supplementary material 8.

In summary, the results above indicate that AOD/AOT and the surface PM_{10} measurements provide related but different information on atmospheric particulates. A myriad of factors cause both PM and AOD vary in complex ways. Conditions in the atmospheric boundary layer (convection and mixing layer height), aerosol size distributions and chemical composition, source regions and transport patterns, and wet scavenging all could result in differences between AOD/AOT and surface aerosol concentration. Further studies to assess the causes of long-term changes in surface PM and AOD as well as the relationships between them appear warranted.

3.7.2 Trends in PM_{10} and AOD

We note that the decreasing trend of PM_{10} level in northern China presented here appears to be different from the trend in visibility over a much longer period (1973–2007, Wang et al., 2009). For the same period as this study (2000 to 2006), Wang et al. found an increase in the AOD in what the authors referred to as the "Asia (south)" region (which includes China, see Fig. 1 in Wang et al., 2009). This is in contrast to the decreasing trend we found for urban PM_{10} in northern China.

What could be the cause of this inconsistency? In fact, the "*Asia (south)*" region in the Wang et al. study includes not only China but also several other countries in southern Asia (Fig. S7 in the supporting online material of Wang et al., 2009, http://www.sciencemag.org/cgi/content/full/323/5920/1468/DC1). It is well known that some of these countries, such as India (Venkataraman et al., 2002), Pakistan (Smith et al., 1996), Bangladesh (Salam et al., 2003) and Vietnam (Deng et al., 2008b), experience severe air pollution. Indeed, the AODs (0.55 µm) derived from visibility measurements at meteorological stations during 2000–2007 were much higher over the southern Asia countries (especially India and Bangladesh) than over China (Fig. S1 in the supporting online material of Wang et al., 2009, http://www.sciencemag.org/cgi/content/full/323/5920/1468/DC1). If the more heavily polluted areas of south Asia were to be excluded from the "*Asia (south)*" region in this analysis, the AOD tendency might well be different. Moreover, emissions (including intensive biomass burning emission) originating in southern Asia also are sources for air pollutants that can be transported across national borders into southwestern China and PRD (Deng et al., 2008b).

On the other hand, as mentioned in Sect. 3.6.2, the PM_{10} trends presented here reflect changes in aerosol loadings in major cities as they were based on APIs of eighty-six major Chinese cities, while the visibility data used in the Wang et al. (2009) study were available for about six hundred sites in mainland China, which were more representative of the variation in air pollution at regional scales. Therefore, the results of these two studies did not necessarily match each other.

More to the point, as discussed above, numerous factors can lead to differences between surface PM_{10} and AOD/AOT. Along these lines, Li et al. (2005) reported that the seasonality of AOD over Urumchi did not precisely follow the monthly variations in common pollutants such as PM_{10}, SO_2 and NO_2. The difference in trends between AOD/AOT and surface PM_{10} could be explained by changes in the emissions of anthropogenic fine particles that have high extinction efficiencies but contribute little to the PM_{10} mass. For example, Zhang et al. (2004) found that the $PM_{2.5}/PM_{10}$ ratio ranged between 0.5–0.7 with an average 0.6 for six cities (Guangzhou, Wuhan, Lanzhou, Chongqing, Qingdao, Beijing) and the PRD in China. High $PM_{2.5}/PM_{10}$ ratios (e.g., larger than 0.6) are generally ascribed to secondary particulate formation; low ratios can be caused by fugitive dusts or dust delivered by long-distance transport (Chan and Yao, 2008).

Various studies also have shown conflicting patterns in AOD. For example, estimates of AOD based on emissions led Streets et al. (2006) to conclude that AOD over China decreased from 1995–1996 (∼0.305) to 2000 (0.29); and this was consistent with variation of surface shortwave irradiance

measurements at fifty-two weather stations and with the rise trend in mean surface temperatures in China starting in the mid-1990s. However, Xia et al. (2007) reported that AOD at 550 nm over Beijing increased from about 0.28 in 1980 to about 0.68 in 2005. Using monthly AOD (500 nm) data from the Total Ozone Mapping Spectrometer (TOMS), Xie and Xia (2008) documented an increasing tendency of AOD in north China from 1997 to 2001, especially for the spring AOD in northeast China. These different results suggested that further investigation on AOD variation trend over China as well as its relationship with surface pollutants such as PM_{10} is needed.

4 Conclusions

A comprehensive analysis of aerosol impacts on climate requires detailed information on chemical composition and optical properties of the aerosol as a function of particle size along with a full set of meteorological measurements. Unfortunately, data of this nature are only available from a few scattered sites and then for limited times over China. Further analysis of the spatial and temporal distribution of the aerosol levels and compositions is obviously necessary to assess its potential effects on climate as well as other effects such as adverse health and visibility impairment. Moreover, information on how the chemical components of the aerosol vary between different locations (e.g. coast and inland) also will be useful.

Most of EPA-China's air quality monitoring stations are located in densely populated urban areas in middle-eastern China, and this makes them suitable for addressing concerns over the health effects of air pollution. However, to study the broader impacts of air pollution, such as climate effects, as well as to evaluate transboundary transport, more monitoring needs to be conducted at rural or remote sites, especially in western China and along the country's borders. In addition, studies of specific types of air pollutants with the potential to influence climate, such as black carbon, sulfate and dust aerosol should be included in the monitoring programs.

Another broad objective for studies involving aerosol particles and their impacts is to link PM loadings to sources. Our studies have shown that spatial distribution of the urban PM_{10} follows the anthropogenic emissions of BC and PM_{10} over much of China but not along the Chinese coast; this suggests that pollutants are diluted by the influx of clean marine air and removed by scavenging of the particles due to more abundant precipitation there.

With further reference to air quality, our data indicate that the urban PM_{10} level in the southern zone may have increased (+12%) from 2000 to 2006, suggesting that additional attention should be paid to the control of atmospheric particulate pollution in southern China. As the secondary aerosol is a major contributor to PM in the southern cities (Ye et al., 2003), controlling emissions of precursor gases may be helpful in improving the air quality in that region.

Decreasing trends in PM_{10} level from 2000 to 2006 suggest improvements in the air quality of major cities in northern China. However, a comparison of the anthropogenic emissions over China between year 2000 and year 2006 shows that the sources for the pollution emissions have become more widely dispersed (see supplementary material 6; Streets et al., 2003; Zhang et al., 2009). The geographical distributions of pollution emissions have been affected by the economic expansion into rural and under-developed areas of China. In addition to stringent controls on large emission sources in urban areas, adequate attention also should be paid to the newer sources in rural and under-developed areas.

The frequencies of Asian dust events mirrored the API maxima for the northern cities, and this indicates that dust can contribute to the degradation of springtime air quality in northern China. Along the same lines, Li et al. (2007) observed important influences of dust events on spring air quality in Shijiazhuang city from 2002 to 2006. In that study, all of the springtime days with mid-level or more serious pollution were concurrent with or followed days of dust-events. Wang et al. (2004b) also reported a significant contribution of Asian dust to PM_{10} pollution at Beijing during the springtime. This is significant because desert dust production will be difficult if not impossible to control, and some allowances for naturally-occurring PM may be appropriate for air quality standards.

Although the PM_{10} dataset as used in this study is not sufficient for an in-depth analysis of aerosol impacts on climate, the results do provide insights into the spatial distributions and temporal variability of the atmospheric aerosol, especially those areas most strongly affected by particulate pollution. Undoubtedly, comparison of infromation on PM obtained using different methods can improve our understanding of the spatio-temporal patterns of the aerosol as well as the potential for climate and other effects. In addition, results of this study will contribute to a better understanding of air pollution in the major urban areas of China, information of this type should be useful for the development and implementation of effective air-pollution control strategies.

Supplementary material related to this article is available online at:
http://www.atmos-chem-phys.net/10/5641/2010/acp-10-5641-2010-supplement.pdf.

Acknowledgements. We are grateful to the anonymous referees for their constructive suggestions and comments. The daily API records for 86 Chinese cities are obtained from State Environmental Protection Agency of China (http://www.sepa.gov.cn/quality/air.php3). This research was supported by National Basic Research Program of China (Grant No. 2006CB403701, 2006CB403702), the Chinese Ministry of

Education's 111 Project (B07036) and by the National Science Foundation of the United States (ATM 0404944).

Edited by: C. K. Chan

References

Bari, A., Ferraro, V., Wilson, L. R., Luttinger, D., and Husain, L.: Measurements of gaseous HONO, HNO_3, SO_2, HCl, NH_3, particulate sulfate and $PM_{2.5}$ in New York, NY, Atmos. Environ., 37(20), 2825–2835, 2003.

Bi, X. H., Feng, Y. C., Wu, J. H., Wang, Y. Q., and Zhu, T.: Source apportionment of PM_{10} in six cities of northern China, Atmos. Environ., 41, 903–912, 2007.

Boersma, K. F., Eskes, H. J., Veefkind, J. P., Brinksma, E. J., van der A, R. J., Sneep, M., van den Oord, G. H. J., Levelt, P. F., Stammes, P., Gleason, J. F., and Bucsela, E. J.: Near-real time retrieval of tropospheric NO2 from OMI, Atmos. Chem. Phys., 7, 2103–2118, doi:10.5194/acp-7-2103-2007, 2007.

Cao, J. J., Lee, S. C., Ho, K. F., Zhang, X. Y., Zou, S. C., Fung, K., Chow, J. C., and Watson, J. G.: Characteristics of carbonaceous aerosol in Pearl River Delta Region, China during 2001 winter period, Atmos. Environ., 37, 1451–1460, 2003.

Chan, C. K. and Yao, X. H.: Air pollution in mega cities in China, Atmos. Environ., 42, 1–42, 2008.

Charlson, R. J., Schwartz, S. E., Hales, J. M., Cess, R. D., Coakley, J. A. J., Hansen, J. E., and Hofmann, D. J.: Climate forcing by anthropogenic aerosols, Science, 255, 423–430, 1992.

Chu, P. C., Chen, Y. C., Lu, S. H., Li, Z. C., and Lu, Y. Q.: Particulate air pollution in Lanzhou China, Environ. Int., 34, 698–713, 2008.

Collins, D. R., Jonsson, H. H., Liao, H., Flagan, R. C., Seinfeld, J. H., Noone, K. J., and Hering, S. V.: Airborne analysis of the Los Angeles aerosol, Atmos. Environ., 34, 4155–4173, 2000.

Davis, B. L. and Guo, J. X.: Airborne particulate study in five cities of China, Atmos. Enviro., 34, 2703–2711, 2000.

Deng, X. J., Tie, X. X., Wu, D., Zhou, X. J., Bi, X. Y., Tan, H. B., Li, F., and Jiang, C. L.: Long-term trend of visibility and its characterizations in the Pearl River Delta (PRD) region, China, Atmos. Environ., 42, 1424–1435, 2008a.

Deng, X. J., Tie, X. X., Zhou, X. J., Wu, D., Zhong, L. J., Tan, H. B., Li, F., Huang, X. Y., Bi, X. Y., and Deng, T.: Effects of Southeast Asia biomass burning on aerosols and ozone concentrations over the Pearl River Delta (PRD) region, Atmos. Environ., 42, 8493–8501, 2008b.

Duan, F. K., He, K. B., Ma, Y. L., Jia, Y. T., Yang, F. M., Lei, Y., Tanaka, S., and Okuta, T.: Characteristics of carbonaceous aerosols in Beijing, China, Chemosphere, 60, 355–364, 2005.

Duan, F. K., He, K. B., Ma, Y. L., Yang, F. M., Yu, X. C., Cadle, S. H., Chan, T., and Mulawa, P. A.: Concentration and chemical characteristics of $PM_{2.5}$ in Beijing, China: 2001–2002, Sci. Total Environ., 355, 264–275, 2006.

Fang, M., Zheng, M., Wang, F., Chim, K. S., and Kot, S. C.: The long-range transport of aerosols from northern China to Hong Kong a multi-technique study, Atmos. Environ., 33, 1803–1817, 1999.

Fang, M., Chan, C. K., and Yao, X. H.: Managing air quality in a rapidly developing nation: China, Atmos. Environ., 43, 79–86, 2009.

Feng, J. L., Hu, M., Chan, C. K., Lau, P. S., Fang, M., He, L. Y., and Tang, X. Y.: A comparative study of the organic matter in $PM_{2.5}$ from three Chinese megacities in three different climatic zones, Atmos. Environ., 40, 3983–3994, 2006.

Guinot, B., Cachier, H., Sciare, J., Tong, Y., Xin, W., and Jianhua, Y.: Beijing aerosol: Atmospheric interactions and new trends, J. Geophys. Res., 112, D14314, doi:10.1029/2006JD008195, 2007.

He, K. B., Yang, F. M., Ma, Y. L., Zhang, Q., Yao, X. H., Chan, C. K., Cadle, S., Chan, T., and Mulawa, P.: The characteristics of $PM_{2.5}$ in Beijing, China, Atmos. Environ., 35, 4959–4970, 2001.

Highwood, E. J. and Kinnersley, R. P.: When smoke gets in our eyes: The multiple impacts of atmospheric black carbon on climate, air quality and health, Environ. Int., 32, 560–566, 2006.

Kaneyasu, N. and Murayama, S.: High concentrations of black carbon over middle latitudes in the North Pacific Ocean, J. Geophys. Res., 105(D15), 19881–19890, 2000.

Kaufman, Y. J., Tanre, D., and Boucher, O.: A satellite view of aerosols in the climate system, Nature, 419, 215–223, 2002.

King, A. M.: New directions: TEOMs and the volatility of UK non-urban PM_{10}: a regulatory dilemma?, Atmos. Environ., 34, 3210–3212, 2000.

Li, S. -M., Tang, J., Xue, H., and Toom-Sauntry, D.: Size distribution and estimated optical properties of carbonate, water soluble organic carbon, and sulfate in aerosols at a remote high altitude site in western China, Geophys. Res. Lett., 27(8), 1107–1110, 2000.

Li, C. C., Mao, J. T., Lau, K. A., Chen, J. C., Yuan, Z. B., Liu, X. Y., Zhu, A. H., and Liu, G. Q.: Characteristics of distribution and seasonal variation of aerosol optical depth in eastern China with MODIS products, Chinese Sci. Bull., 48(22), 2488–2495, 2003.

Li, X., Chen, Y. H., Hu, X. Q., Ren, Y. Y., and Wei, W. S.: Analysis of atmospheric aerosol optical properties over Urumqi, China Environmental Science, 25(supp.), (in Chinese with English abstract), 22–25, 2005.

Li, Y., Zhang, X. Y., Gong, S. L., Che, H. Z., Wang, D., Qu, W. J., and Sun, J. Y.: Comparison of EC and BC and evaluation of dust aerosol contribution to light absorpition in Xi'An, China, Environ. Monit. Assess., 120, 301–312, 2006.

Li, G. C., Wang, J. G., and Lian, Z. L.: Relationship between atmospheric pollution and sandy weather in Shijiazhuang, (in Chinese with English abstract), J. Meteorol. Environ., 23(2), 1–5, 2007.

Li, J., Zhuang, G. S., Huang, K., Lin, Y. F., Xu, C., and Yu, S. L.: Characteristics and sources of air-borne particulate in Urumqi, China, the upstream area of Asia dust, Atmos. Environ., 42, 776–787, 2008.

Luo, Y. F., Lü, D. R., He, Q., Li, W. L., and Zhou, X. J.: Characteristics of atmospheric aerosol optical depth variation over China in recent 30 years, Chinese Sci. Bull., 45(14), 1328–1333, 2000.

Luo, Y., Lu, D., Zhou, X., Li, W., and He, Q.: Characteristics of the spatial distribution and yearly variation of aerosol optical depth over China in last 30 years, J. Geophys. Res., 106(D13), 14501–14513, 2001.

Meng, Z. Y., Jiang, X. M., Yan, P., Lin, W. L., Zhang, H. D., and Wang, Y.: Characteristics and sources of $PM_{2.5}$ and carbonaceous species during winter in Taiyuan, China, Atmos. Environ., 41, 6901–6908, 2007.

Met One Instruments Inc: BAM-1020 continuous particulate monitor: http://www.metone.com/documents/BAM-1020_6-08.pdf, last access: 28 August 2009.

Meywerk, J. and Ramanathan, V.: Observations of the spectral clear-sky aerosol forcing over the tropical Indian Ocean, J. Geophys. Res., 104(D20), 24359–24370, 1999.

Mo, Y. C., Zheng, F. Q., and Liao, G. L.: Correlation analysis of PM_{10} concentration and meteorological condition in Nanning, (in Chinese with English abstract), J. Meteorol. Res. Appl., 29(1), 55–56, 2008.

Nair, V. S., Babu, S. S., and Moorthy, K. K.: Aerosol characteristics in the marine atmospheric boundary layer over the Bay of Bengal and Arabian Sea during ICARB: Spatial distribution and latitudinal and longitudinal gradients, J. Geophys. Res., 113, D15208, doi:10.1029/2008JD009823, 2008.

National Bureau of Statistics of China: China Statistical Yearbook 2005, China Statistics Press, Beijing, China, 2005a.

National Bureau of Statistics of China: Urban Statistical Yearbook of China 2005, China Statistics Press, Beijing, China, 2005b.

National Bureau of Statistics of China: China Statistical Yearbook 2006, China Statistics Press, Beijing, China, 2006a.

National Bureau of Statistics of China: Urban Statistical Yearbook of China 2006, China Statistics Press, Beijing, China, 2006b.

National Bureau of Statistics China: http://www.stats.gov.cn/tjsj/ndsj/2007/indexch.htm, access: 28 April 2010.

Ning, H. W., Wang, S. G., and Du, J. W.: Characteristics of sand-dust events and their influence on air quality of Xi'an city, (in Chinese with English abstract), J. Desert Res., 25(6), 886–890, 2005.

Okuda, T., Kato, J., Mori, J., Tenmoku, M., Suda, Y., Tanaka, S., He, K. B., Ma, Y. L., Yang, F. M., Yu, X. C., Duan, F. K., and Lei, Y.: Daily concentrations of trace metals in aerosols in Beijing, China, determined by using inductively coupled plasma mass spectrometry equipped with laser ablation analysis, and source identification of aerosols, Sci. Total Environ., 330, 145–158, 2004.

Okuda, T., Katsuno, M., Naoi, D., Nakao, S., Tanaka, S., He, K. B., Ma, Y. L., Lei, Y., and Jia, Y. T.: Trends in hazardous trace metal concentrations in aerosols collected in Beijing, China from 2001 to 2006, Chemosphere, 72, 917–924, 2008.

Pope, C. A., Dockery, D. W., and Schwartz, J.: Review of epidemiological evidence of health effects of particulate air pollution, Inhal. Toxicol., 7, 1–18, 1995.

Qu, W. J., Zhang, X. Y., Arimoto, R., Wang, D., Wang, Y. Q., Yan, L. W., and Li Y.: Chemical composition of the background aerosol at two sites in southwestern and northwestern China: potential influences of regional transport, Tellus, 60B, 657–673, 2008.

Rajeev, K. and Ramanathan, V.: Direct observations of clear-sky aerosol radiative forcing from space during the Indian Ocean Experiment, J. Geophys. Res., 106(D15), 17221–17235, 2001.

Salam, A., Bauer, H., Kassin, K., Ullah, S. M., and Puxbaum, H.: Aerosol chemical characteristics of a mega-city in Southeast Asia (Dhaka-Bangladesh), Atmos. Environ., 37, 2517–2528, 2003.

Sciare, J., Cachier, H., Sarda-Estève, R., Yu, T., and Wang, X.: Semi-volatile aerosols in Beijing (R.P. China): Characterization and influence on various $PM_{2.5}$ measurements, J. Geophys. Res., 112, D18202, doi:10.1029/2006JD007448, 2007.

Shao, M., Tang, X. Y., Zhang, Y. H., and Li, W. J.: City clusters in China: air and surface water pollution, Front. Ecol. Environ., 4(7), 353–361, 2006.

Shi, C. E., Zhai, W. Q., Yang, J., Wang, S., and Yao, K. Y.: Characteristics of PM_{10} pollution at four provincial cities in Yangtze River Delta district, (in Chinese with English abstract), Plateau Meteorol., 27(2), 408–414, 2008.

Smith, D. J. T., Harrision, R. M., Luhana, L., Casimiro, A. P., Castro, L. M., Tariq, M. N., Hayat, S., and Quraishi, T.: Concentrations of particulate airborne polycyclic aromatic hydrocarbons and metals collected in Lahore, Pakistan, Atmos. Environ., 30, 4031–4040, 1996.

Song, Y., Tang, X. Y., Zhang, Y. H., Hu, M., Fang, C., Zen, L. M., and Wang W.: Effects on fine particles by the continued high temperature weather in Beijing, (in Chinese with English abstract), Environ. Science, 23(4), 33–36, 2002.

Song, C. -K., Ho, C. -H., Park, R. J., Choi, Y. -S., Kim, J., Gong, D. Y., and Lee, Y. -B.: Spatial and seasonal variations of surface PM_{10} concentration and MODIS aerosol optical depth over China, Asia-Pacific Journal of Atmospheric Sciences, 45(1), 33–43, 2009.

Streets, D. G., Bond, T. C., Carmichael, G. R., Fernandes, S. D., Fu, Q., He, D., Klimont, Z., Nelson, S. M., Tsai, N. Y., Wang, M. Q., Woo, J. -H., and Yarber, K. F.: An inventory of gaseous and primary aerosol emissions in Asia in the year 2000, J. Geophys. Res., 108(D21), 8809, doi:10.1029/2002JD003093, 2003.

Streets, D. G., Yu, C., Wu, Y., Chin, M., Zhao, Z. C., Hayasaka, T., and Shi, G. Y.: Did Aerosols over China peak in the 1990s?, discussion paper of Global Environment and Energy in the 21st Century: available online at: http://www.gee-21.org/publications/Aerosols-over-China.pdf, 2006.

Ta, W. Q., Wang, T., Xiao, H. L., Zhu, X. Y., and Xiao, Z.: Gaseous and particulate air pollution in the Lanzhou Valley, China, Sci. Total Environ., 320, 163–176, 2004.

Tang, J., Wen, Y. P., Zhou, L. X., Qi, D. L., Zheng, M., Trivett, N., and Wallgren, E.: Observational study of black carbon in clean air area of western China, (in Chinese with English abstract), Q. J. Appl. Meteorol., 10(2), 160–170, 1999.

The Climate Source, Inc.: PRISM 1961–1990 mean annual precipitation mainland China, http://www.climatesource.com/cn/fact_sheets/chinappt_xl.jpg, last access: 19 April 2010.

Tie, X. X., Brasseur, G. P., Zhao, C. S., Granier, C., Massie, S., Qin, Y., Wang, P. C., Wang, G. L., Yang, P. C., and Richter, A.: Chemical characterization of air pollution in Eastern China and the Eastern United States, Atmos. Environ., 40, 2607–2625, 2006a.

Tie, X. X., Li, G. H., Ying, Z. M, Guenther, A., and Madronich, S.: Biogenic emissions of isoprenoids and NO in China and comparison to anthropogenic emissions, Sci. Total Environ., 371, 238–251, 2006b.

Tie, X. X., and Cao, J. J.: Aerosol pollution in China: Present and future impact on environment, Particuology, 7, 426–431, 2009a.

Tie, X. X., Wu, D., and Brasseur, G.: Lung cancer mortality and exposure to atmospheric aerosol particles in Guangzhou, China, Atmos. Environ., 43, 2375–2377, 2009b.

Turpin, B. J., Saxena, P., and Andrews, E.: Measuring and simulating particulate organics in the atmosphere: problems and prospects, Atmos. Environ., 34, 2983–3013, 2000.

Twomey, S.: The influence of pollution on the short-wave albedo of clouds, J. Atmos. Sci., 34, 1149–1152, 1977.

Venkataraman, C., Reddy, C. K., Josson, S., and Reddy, M. S.: Aerosol size and chemical characteristics at Mumbai, India, dur-

ing the INDOEX-IFP (1999), Atmos. Environ., 36, 1979–1991, 2002.

Wang, T., Wong, C. H., Cheung, T. F., Blake, D. R., Arimoto, R., Baumann, K., Tang, J., Ding, G. A., Yu, X. M., Li, Y. S., Streets, D. G., and Simpson, I. J.: Relationships of trace gases and aerosols and the emission characteristics at Lin'an, a rural site in eastern China, during spring 2001, J. Geophys. Res., 109, D19S05, doi:10.1029/2003JD004119, 2004a.

Wang, Y. Q., Zhang, X. Y., Arimoto, R., Cao, J. J., and Shen, Z. X.: The transport pathways and sources of PM_{10} pollution in Beijing during spring 2001, 2002 and 2003, Geophys. Res. Lett., 31, L14110, doi:10.1029/2004GL019732, 2004b.

Wang, S. G., Wei, Y., and Shang, K. Z.: The impacts of different kinds of dust events on PM_{10} pollution in northern China, Atmos. Environ., 40, 7975–7982, 2006.

Wang, Y., Xin, J., Li, Z., Wang, S., Wang, P., Hao, W. M., Nordgren, B. L., Chen, H., Wang, L., and Sun, Y.: Seasonal variations in aerosol optical properties over China, Atmos. Chem. Phys. Discuss., 8, 8431–8453, 2008,

Wang, K. C., Dickinson, R. E., and Liang, S. L.: Clear sky visibility has decreased over Land globally from 1973 to 2007, Science, 323, 1468–1470, 2009.

Watson, J.: Visibility: Science and regulation, J. Air Waste Manage. Assoc., 52, 628–713, 2002.

Wen, X. H., He, P., Li, C. Z., and Luo, X. Y.: Pollution level of the airborne particulate matter (PM_{10}) in Nanchong City, (in Chinese with English abstract), Sichuan Environ., 23(2), 72–74, 2004.

Wu, D., Tie, X. X., Li, C. C., Ying, Z. M., Lau, A. K., Huang, J., Deng, X. J., and Bi, X. Y.: An extremely low visibility event over the Guangzhou region: A case study, Atmos. Environ., 39, 6568–6577, 2005.

Xia, X. A., Chen, H. B., Wang, P. C., Zhang, W. X., Goloub, P., Chatenet, B., Eck, T. F., and Holben, B. N.: Variation of column-integrated aerosol properties in a Chinese urban region, J. Geophys. Res., 111, D05204, doi:10.1029/2005JD006203, 2006.

Xia, X., Chen, H., Goloub, P., Zhang, W., Chatenet, B., and Wang P.: A compilation of aerosol optical properties and calculation of direct radiative forcing over an urban region in northern China, J. Geophys. Res., 112, D12203, doi:10.1029/2006JD008119, 2007.

Xia, D. S., Chen, F. H., Bloemendal, J., Liu, X. M., Yu, Y., and Yang, L. P.: Magnetic properties of urban dustfall in Lanzhou, China, and its environmental implications, Atmos. Environ., 42, 2198–2207, 2008.

Xie, J. X. and Xia, X. A.: Long-term trend in aerosol optical depth from 1980 to 2001 in north China, Particuology, 6, 106–111, 2008.

Xu, J., Bergin, M. H., Yu, X., Liu, G., Zhao, J., Carrico, C. M., and Baumann, K.: Measurement of aerosol chemical, physical and radiative properties in the Yangtze delta region of China, Atmos. Environ., 36, 161–173, 2002.

Yao, Q., Li, S. Q., Xu, H. W., Zhuo, J. K., and Song, Q.: Studies on formation and control of combustion particulate matter in China: A review, Energy, 34(9), 1296–1309, 2009.

Ye, B. M., Ji, X. L., Yang, H. Z., Yao, X. H., Chan, C. K., Cadle, S. H., Chan, T., and Mulawa, P. A.: Concentration and chemical composition of $PM_{2.5}$ in Shanghai for a 1-year period, Atmos. Environ., 37(4), 499–510, 2003.

Zhang, X. Y., Cao, J. J., Li, L. M., Arimoto, R., Cheng, Y., Huebert, B., and Wang, D.: Characterization of atmospheric aerosol over XiAn in the South Margin of the Loess Plateau, China, Atmos.Environ., 36, 4189–4199, 2002.

Zhang, X. Y., Gong, S. L., Shen, Z. X., Mei, F. M., Xi, X. X., Liu, L. C., Zhou, Z. J., Wang, D., Wang, Y. Q., and Cheng, Y.: Characterization of soil dust aerosol in China and its transport/distribution during 2001 ACE-Asia: 1. Network observations, J. Geophys. Res., 108(D9), 4261, doi:10.1029/2002JD002632, 2003.

Zhang, Y. H., Zhu, X. L., Slanina, S., Shao, M., Zeng, L. M., Hu, M., Bergin, M., and Salmon, L.: Aerosol pollution in some Chinese cities (IUPAC Technical Report), Pure Appl. Chem., 76(6), 1227–1239, 2004.

Zhang, X. Y., Wang, Y. Q., Wang, D., Gong, S. L., Arimoto, R., Mao, L. J., and Li, J.: Characterization and sources of regional-scale transported carbonaceous and dust aerosols from different pathways in coastal and sandy land areas of China, J. Geophys. Res., 110, D15301, doi:10.1029/2004JD005457, 2005.

Zhang, X. M., Chai, F. H., Wang, S. L., Hu, B. Q., Li, K., and Luo, L. B.: Characteristics of air pollution in Shenyang city, China, (in Chinese with English abstract) China Environ. Sci., 26(6), 650–652, 2006.

Zhang, B. L., Tsunekawa, A., and Tsubo, M.: Contributions of sandy lands and stony deserts to long-distance dust emission in China and Mongolia during 2000–2006, Global Planet. Change, 60, 487–504, 2008.

Zhang, Q., Streets, D. G., Carmichael, G. R., He, K. B., Huo, H., Kannari, A., Klimont, Z., Park, I. S., Reddy, S., Fu, J. S., Chen, D., Duan, L., Lei, Y., Wang, L. T., and Yao, Z. L.: Asian emissions in 2006 for the NASA INTEX-B mission, Atmos. Chem. Phys., 9, 5131–5153, 2009, http://www.atmos-chem-phys.net/9/5131/2009/.

Zheng, M., Salmon, L. G., Schauer, J. J., Zeng, L. M., Kiang, C. S., Zhang, Y. H., and Cass, G. R.: Seasonal trends in $PM_{2.5}$ source contributions in Beijing, China, Atmos. Environ., 39(22), 3967–3976, 2005.